310–327 *Nucleic Acids Research, 2019, Vol. 47, No. 1* *Published online 8 November 2018*
doi: 10.1093/nar/gky1109

RNA polymerase III subunits C37/53 modulate rU:dA hybrid 3′ end dynamics during transcription termination

Saurabh Mishra[1] and Richard J. Maraia[1,2,*]

[1]Intramural Research Program of the *Eunice Kennedy Shriver* National Institute of Child Health and Human Development, National Institutes of Health, Bethesda, MD 20892, USA and [2]Commissioned Corps, U.S. Public Health Service, Rockville, MD 20852, USA

Received July 11, 2018; Revised October 04, 2018; Editorial Decision October 19, 2018; Accepted October 22, 2018

ABSTRACT

RNA polymerase (RNAP) III synthesizes tRNAs and other transcripts, and mutations to its subunits cause human disorders. The RNAP III subunit-heterodimer C37/53 functions in initiation, elongation and in termination-associated reinitiation with subunit C11. C37/53 is related to heterodimers associated with RNAPs I and II, and C11 is related to TFIIS and Rpa12.2, the active site RNA 3′ cleavage factors for RNAPs II and I. Critical to termination is stability of the RNA:DNA hybrid bound in the active center, which is loose for RNAP III relative to other RNAPs. Here, we examined RNAP III lacking C37/53/C11 and various reconstituted forms during termination. First, we established a minimal terminator as 5T and 3A on the non-template and template DNA strands, respectively. We demonstrate that C11 stimulates termination, and does so independently of its RNA cleavage activity. We found that C37/53 sensitizes RNAP III termination to RNA:DNA hybrid strength and promotes RNA 3′ end pairing/annealing with the template. The latter counteracts C11-insensitive arrest in the proximal part of the oligo(T)-tract, promoting oligo(rU:dA) extension toward greater hybrid instability and RNA release. The data also indicate that RNA 3′ end engagement with the active site is a determinant of termination. Broader implications are also discussed.

INTRODUCTION

tRNAs are produced at 10- to 12-fold molar excess relative to ribosomes to support efficient mRNA translation (1). Specialization of RNAP III for large amounts of short transcripts such as tRNAs reflects high efficiency transcription (2) and a process known as facilitated recycling, involving proficient transition from termination to reinitiation (3). RNAP III achieves this with stably associated subunit complexes that are homologous to dissociable transcription factors (TFs) used by RNAP II (2,4). RNAP III initiation-specific subunit heterotrimer, C31/34/82 is related to TFIIEα/β (5,6) while the heterodimer C37/53 is related to TFIIFα/β, and the RNAP I subunit heterodimer 49/34.5 (7,8). C37/53 and subunit C11 together promote facilitated recycling (9). The C11 NTD is similar to RNAP II subunit, Rpb9 while its CTD is homologous to the RNAP II ancillary elongation factor, TFIIS and the RNAP I subunit Rpa12.2, and confers RNAP-associated RNA 3′ cleavage activity similar to both (10–12).

RNAP III is controlled by its repressor, Maf1 and the TOR complex in response to nutrient signaling to maintain metabolic economy and is also linked to organismal longevity (13–16). In addition, cytoplasmic RNAP III is the primary target DNA sensor of viral infection that signals an important innate immune response (17,18). Data indicate that in this activity, RNAP III mediates promoter-independent transcription initiation, consistent with lack of requirement for its initiation-specific subunits (18). Furthermore, a multitude of hereditary mutations in other RNAP III subunits underlie defects in this pathway and account for severe pathogenic responses to otherwise self-limited childhood viral infections (19,20). A plethora of recessive mutations in the two largest RNAP III subunits, C1 and C2 (POLR3A and POLR3B) underlie a distinct childhood neurologic dysfunction syndrome known as POLR3-related leukodystrophy (21,22).

Human C53 was cloned as a gene that complements a temperature-sensitive cell cycle mutant of baby hamster kidney cells as the first identified subunit of human RNAP III (23). Notably, mutations in POLR3E, the human homolog of C37, cause failure in cytoplasmic Pol III DNA sensing and severe outcomes to viral infections (20). Notably, at initiation, C37/53 contributes to promoter opening, and at elongation, C53 was shown to crosslink to the RNA 3′ end

*To whom correspondence should be addressed. Tel: +1 301 402 3567; Fax: +1 301 496 0243; Email: maraiar@mail.nih.gov
Disclaimer: The funders had no role in study design, data collection and interpretation, or the decision to submit the work for publication.

(24). Protein-protein crosslinking localized a CTD-loop region of C37 to the RNAP III active center (25). Better insight into how RNAP III coordinates these activities is key to understanding mechanistic aspects of its function and the mutations that effect dysfunction.

Consistent with crosslinking data, high-resolution structures show that while the major mass of C37/53/11 reside at the RNAP III periphery, other parts reach into the active center (26–28). Yeast RNAP III that lacks C37/53 and C11 (pol IIIΔ) exhibits increased elongation rate and is defective for termination (9,10), similar to other 'kinetic coupling' mutants that read-through the oligo(dT) terminators of RNAP III-transcribed genes (29,30).

Notably, recombinant C37/53 could reconstitute a termination deficiency of pol IIIΔ without addition of C11 (9). Intriguingly however, C37/53 plus C11 is required for facilitated recycling, although the RNA 3′ cleavage activity of the latter is not (9). Genetic data suggest involvement of the CTD and the NTD of C11 in termination *in vivo* (26,31–33). Yet, while ample biochemical evidence has further indicated that C37/53 is major factor that promotes RNAP III termination (34,35), clear biochemical evidence of C11 activity in termination *per se* has remained elusive.

Elongation complexes (ECs) assembled on DNA–RNA scaffolds showed that pol IIIΔ, hereafter referred to as 'RNAP III-core', can terminate efficiently if provided a long enough oligo(dT) tract, but does so only at the distal end of a 9T tract, whereas the RNAP-holoenzyme terminates in the proximal part of the 9T tract (34). It has long been known that oligo(rU:dA) is far more unstable than any other duplex (36), and that the overall stability of the RNA:DNA hybrid is a major determinant of transcription termination (37). Thus, the previous data (34) led to the hypothesis that a relatively long oligo(rU:dA) of 8–9 basepairs is required to provide sufficient destabilization of the RNA:DNA hybrid for termination in the absence of C37/53.

Recent data revealed oligo(dT) as a sequence-specific (T3-T4-T5) non-template (NT) pause-terminator element that promotes proximal termination in conjunction with the C37-CTD-loop but did not examine a role for the rU:dA hybrid (35). A cryo-EM EC structure resolved the C37-CTD-loop near the NT strand (26). The same study documented an active center with unusually loose fit around the RNA:DNA hybrid as compared to other RNAPs, raising the hypothesis that relaxed hybrid binding may be relevant to the unique mechanism of efficient termination by RNAP III (26,38,39).

Although it was known that a fraction of RNAP III-core specifically has some propensity to arrest in the proximal part of a 9T tract, the mechanism was unknown (34). It was speculated that a backtracked state in which the RNA 3′ end is extruded from the catalytic site is a likely intermediate of termination by RNAP III (39). Relevant to this, the RNA 3′ cleavage-active form of C11 added to RNAP III-core as an isolated subunit did not promote termination or relieve arrest, whereas addition of C37/53 subunits did (34,35). A model of deep backtracking by RNAP III into an oligo(T)-proximal hairpin was disproven as necessary for termination *in vitro* and *in vivo* (40). However, effects of other types of RNA 3′ end disengagement with the active site on termination have not been examined. Here, we used RNAP III ECs to first define a minimal terminator for *in vitro* termination assays. We show that C11 stimulates C37/53-dependent termination using this system, but that this is independent of its RNA 3′ cleavage activity. Additionally, we uncovered a new activity for C37/53; it exacerbates effects of RNA:DNA hybrid instability on termination. We provide key evidence that C37/53 helps retain the RNA 3′ end aligned/annealed with the template strand in the active site during elongation preceding termination and at termination. The collective data lead to a new model of termination that accounts for these activities and the loose RNA:DNA hybrid-binding active site of RNAP III.

MATERIALS AND METHODS

Oligos were purchased from Integrated DNA Technologies or Eurofins Genomics and listed in Table 1. Nucleotide triphosphates (NTPs) were from Thermo-Scientific. 5-bromo-UTP (BrU) and 4-Thio UTP (4sU, sU) was from Sigma and TriLink BioTechnologies, respectively.

RNAP III purification

RNAP III was purified as described (34) from a *Saccharomyces cerevisiae* strain carrying an N-His-FLAG-tagged RPC128 (C128) gene, and RNAP III-core was purified from a strain carrying N-His-FLAG C128 in which RPC11 was deleted and complemented with *Schizosaccharomyces pombe* C11 (24). Briefly, 40 g of cells were lysed by bead beater in ice-cold lysis buffer (40 mM Na-HEPES, pH 7.8, 5% glycerol, 10 mM 2-mercaptoethanol, 0.5 M NaCl, 7 mM $MgCl_2$ and protease inhibitors). Supernatant was collected after centrifugation in a Sorvall SLA-1500 rotor at 12 000 rpm for 30 min and then again subjected to ultracentrifugation (Beckman) at 38 000 rpm in a 60 Ti rotor for 1 h at 4°C. The top layer was recovered (S100), avoiding the murky layer above the pellet. The S100 was incubated with Ni-NTA resin (Qiagen) at 4°C. RNAP III was eluted with 20 mM Na HEPES, pH 8, 20% glycerol, 500 mM NaCl, 10 mM 2-mercaptoethanol, 7 mM $MgCl_2$, 100 mM imidazole and complete protease inhibitor (Roche). Small aliquots were stored at −70°C.

RNAP III subunit expression and purification

C11 and the C37/53 recombinant heterodimer were purified as previously described (34). For C11-WT and the C11-MT ($C11^{AA}$), pGEX-4T-1 plasmids containing C11 and C11-D91A.E92A were transformed and expressed in Rosetta (DE3) pLysS cells with 100 μM Isopropyl β-D-1-thiogalactopyranoside (IPTG) for 3 h at 37°C. Cells were lysed in lysis buffer (50 mM K-HEPES, pH 7.8, 500 mM NaCl, 5% glycerol, 10 mM 2-mercaptoethanol, 1%Triton X-100, and protease inhibitors) and then centrifuged at 12 000 rpm at 4°C for 30 min. Supernatant was incubated with glutathione-Sepharose (GE Healthcare), equilibrated and washed with lysis buffer, and then with wash buffer (WB; 20 mM K- HEPES, pH 7.8, 200 mM NaCl, 10% glycerol, 10 mM 2-mercaptoethanol). Protein was eluted by digestion with thrombin at 4°C overnight in WB. In total, 2 mM

Table 1. List of all DNA and RNA oligonucleotides used

Name	Sequence (5′ to 3′)	Terminator	Strand	Remarks
AGTO7	AACAATTAAATACTCTCTATTATCCATA GGCGGACGACGAAAGGCGCAAGACTTTT TTTTTGTCTCCAAGACTTGCTCGC	9T	NT	
AGTO16	GCGAGCAAGTCTTGGAGACAAAAAAA AAGTCTTGCGCCTTTCGTCGTCCGCCTA TGGATAATAGAGAGTATTTAATTGTT	9T	T	
SMO27X	AACAATTAAATACTCTCTATTATCCATA GGCGGACGACGAAAGGCGCAAGACTTTT TAGAAGTCTCCAAGACTTGCTCGC	5T	NT	For minimal terminator
SMO77	GCGAGCAAGTCTTGGAGACTTCTAAAAA GTCTTGCGCCTTTCGTCGTCCGCCTATG GATAATAGAGAGTATTTAATTGTT	5A	T	for 5T-5A terminator
SMO31X	GCGAGCAAGTCTTGGAGACTTCTTTAAA GTCTTGCGCCTTTCGTCGTCCGCCTATG GATAATAGAGAGTATTTAATTGTT	3A	T	For 5T-3A minimal terminator
SMO8	GCGAGCAAGTCTTGGAGACTTTTTAAAA GTCTTGCGCCTTTCGTCGTCCGCCTATG GATAATAGAGAGTATTTAATTGTT	4A	T	for 5T-4A terminator
SMO78	GCGAGCAAGTCTTGGAGACTTCTTTTAA GTCTTGCGCCTTTCGTCGTCCGCCTATG GATAATAGAGAGTATTTAATTGTT	2A	T	for 5T-2A terminator
SMO73	AACAATTAAATACTCTCTATTATCCATA GGCGGACGACGAAAGGCGCAAGACTA TTTAGAAGTCTCCAAGACTTGCTCGC	5T	NT	T2A substitution within 5Ts stretch
SMO74	AACAATTAAATACTCTCTATTATCCATA GGCGGACGACGAAAGGCGCAAGACTT ATTAGAAGTCTCCAAGACTTGCTCGC	5T	NT	T3A substitution within 5Ts stretch
SMO75	AACAATTAAATACTCTCTATTATCCATA GGCGGACGACGAAAGGCGCAAGACTT TATAGAAGTCTCCAAGACTTGCTCGC	5T	NT	T4A substitution within 5Ts stretch
AGTO31	AACAATTAAATACTCTCTATTATCCATA GGCGGACGACGAAAGGCGCAAGACTTTT TTGTCTCCAAGACTTGCTCGCAGC	T6	NT	6T terminator
AGTO32	GCTGCGAGCAAGTCTTGGAGACAAAAAA GTCTTGCGCCTTTCGTCGTCCGCCTATG GATAATAGAGAGTATTTAATTGTT	6A	T	6T terminator
SMO124	AACAATTAAATACTCTCTATTATCCATA GGCGGACGACGAAAGGCGCAAAACTTTT TAGAAGTCTCCAAGACTTGCTCGC	5T	NT	20% G-C content upstream of 5Ts terminator
SMO125	GCGAGCAAGTCTTGGAGACTTCTAAAAA GTTTTGCGCCTTTCGTCGTCCGCCTATG GATAATAGAGAGTATTTAATTGTT	5A	T	20% G-C content upstream of 5As terminator
SMO126	AACAATTAAATACTCTCTATTATCCATA GGCGGACGACGAAAGGCGCAAAAATT TTTAGAAGTCTCCAAGACTTGCTCGC	5T	NT	0% G-C content upstream of 5As terminator
SMO127	GCGAGCAAGTCTTGGAGACTTCTAAAAA TTTTTGCGCCTTTCGTCGTCCGCCTATG GATAATAGAGAGTATTTAATTGTT	5A	T	0% G-C content upstream of 5As terminator
SMO128	AACAATTAAATACTCTCTATTATCCATA GGCGGACGACGAAAGGCGCACGACTTTT TAGAAGTCTCCAAGACTTGCTCGC	5T	NT	60% G-C content upstream of 5As terminator
SMO129	GCGAGCAAGTCTTGGAGACTTCTAAAAA GTCGTGCGCCTTTCGTCGTCCGCCTATG GATAATAGAGAGTATTTAATTGTT	5A	T	60% G-C content upstream of 5As terminator
SMO142	AACAATTAAATACTCTCTATTATCCATA GGCGGACGACGAAAGGCGCACCCCTTTT TAGAAGTCTCCAAGACTTGCTCGC	5T	NT	First 4 nucleotides of terminator NT strand substituted with A
SMO109	AACAATTAAATACTCTCTATTATCCATA GGCGGACGACGAAAGGTGTAAGAGAA GGTGGAAGAGGTTTTCCCCAGTCTCCAA GACTTGCTCGC	4T	NT	For Figure 4A
SMO110	GCGAGCAAGTCTTGGAGACTGGGGAA AACCTCTTCCACCTTCTCTTACACCTTTCG TCGTCCGCCTATGGATAATAGAGAGTAT TTAATTGTT	4A	T	For Figure 4A
RNA1	CGGACGACGA			RNA primer for making transcription assembly
RNA6	CGGACGACGAUU			RNA was used for cleavage assay

NT and T in the 'strand' column indicate NT and template strands, respectively.

benzamidine–HCl was added to inactivate thrombin, and the purified proteins were stored frozen at −70°C.

For C37/53 recombinant heterodimer, pET28-nH6TEVC53 was cotransformed along with pET21-nFLAGC37 and plated on LB media containing ampicillin (100 g/ml) and kanamycin (50 g/ml) and induced with 0.5 mM IPTG. Cells were lysed in lysis buffer (50 mM Na-HEPES, pH 8, 200 mM NaCl, 5% glycerol, 10 mM 2-mercaptoethanol and protease inhibitors) and centrifuged at 12 000 rpm and supernatant was collected and passed through Ni-NTA resin (Qiagen), and the complex was eluted with 20 mM K-HEPES, pH 8, 200 mM NaCl, 10 mM 2-mercapto- ethanol, 10% glycerol 300 mM imidazole. Peak fractions were pooled, 40 unit of Turbo TEV protease (Eaton Biosciences Inc.) was added, and the mix was dialyzed against elution buffer lacking imidazole. Samples were again passed through Ni-NTA to remove unwanted tagged fragments and undigested proteins and the flowthrough was passed through an SP Sepharose (GE Healthcare) column equilibrated with dialysis buffer using the ÄKTA purifier system (GE Amersham). Peak fractions were pooled, and buffer (20 mM Tris–Cl, pH 8, 200 mM NaCl, 10 mM 2-mercaptoethanol, 10% glycerol and protease inhibitors) was exchanged using a PD10 column (GE Healthcare) using the ÄKTA system. Finally, the C53/37 complexes were applied to a Q-Sepharose (GE Healthcare) column and eluted with 300 mM NaCl.

For purification of C37/53*, pET28-nH6TEVC53-Nt (amino acids 2–280 deleted) (34) was cotransformed along with pET21-nFLAGC37 into Rosetta (DE3) pLysS and the resulting heterodimer was purified as above using the ÄKTA system (GE Amersham).

Cloning of C37* (containing five alanine substitution at positions 226–230) was by Q5® Site-Directed Mutagenesis Kit (NEB) using pET21-nFLAGC37 as template. For C37*/53 purification, pET21-nFLAGC37* was cotransformed with pET28-nH6TEVC53 into Rosetta (DE3) pLysS and the C37*/53 heterodimer was purified as described above.

EC assembly and transcriptions

EC assembly on scaffolds and transcription reactions were as described (35). The EC with a 2 nt 3′ overhang employed for Figure 7B used template AGO16, RNA6 and NT AGO 7. 6His-tagged RNAP III was immobilized on magnetic Ni-NTA beads (Thermo-scientific), washed with EC buffer (ECB; 20 mM Na-HEPES, pH 8, 3 mM β-mercaptoethanol, 5% glycerol, 0.1 mg/ml bovine serum albumin, 100 mM NaCl). 1 μM T-DNA and 1 μM 5′-end-labeled ^{32}P-RNA were added and annealed in ECB by heating to 55°C and rapid cooling to room temp. This was incubated with immobilized RNAP III for 10 min at room temperature. A total of 2 μM NT-DNA was added and incubated for 10 min, followed by three washes with ECB. For all experiments, equal amounts of RNAP III-holo and RNAP III-core transcription activities were used. A typical 1× reaction contained 50 μl of beads. For some experiments, a larger batch of ECs were prepared and washed then aliquotted into equal smaller volumes for subsequent analysis.

For reconstitutions of RNAP III, recombinant proteins (Supplementary Figure S1) were incubated with the ECs for 10 min prior to NTP addition. For all RNAP III reconstitutions, the same amounts (1000 ng, a large molar excess) of recombinant proteins were used and this was consistent across all experiments. A total of 500 μM NTPs containing 7 mM MgCl2 was added and incubated for 10 min at room temperature followed by separation of released from bound by magnet and immediate phenol extraction/ethanol precipitation. Samples were dissolved in formamide with dye, resolved on 15% sequencing gels, dried, exposed to phosphorimager screen and visualized using Typhoon (GE Healthcare). Reactions were stopped at indicated times by phenol extraction followed by ethanol precipitation and analyzed by 15% denaturing urea-polyacrylamide gel electrophoresis.

Isolation and chase of sU complexes

After assembly as described above the ECs were extended with a mixture of 100 μM each of 4sUTP, CTP, ATP, GTP for 3 min followed by four washes, each equal to the bead volume, with ECB. Chase was with ECB and/or with recombinant proteins and/or 500 μM each UTP/CTP/ATP/GTP and incubation for 30 min. For chase experiments, a batch of ECs were prepared then aliquotted into smaller volumes for subsequent analysis.

TE was calculated as follows

TE (%) = (RNA released at terminator/Total RNA) × 100. Total = RNA released in TZ + released RT RNA + bound at TZ + bound at RT); the abbreviations TZ refers to terminator zone (TZ) and RT refers to readthrough. TE, where indicated, were derived from triplicate experiments, shown as standard deviation (SD). For some experiments, '% release' was derived from duplicate experiments and shown as standard error SE (SE = SD/$\sqrt{}$ n) as indicated in the figure legends.

For analysis using the TE_Q method, half of the released material (R) from a reaction was loaded in one lane. The other half of the released material (R) plus all of the material from the bound fraction (B) of the reaction, denoted as R+B, was loaded in the adjacent lane. TE_Q was calculated after quantitation as TE_Q = (2R)/[(R) + (R+B)] x 100.

Quantifications

Image files were analyzed for densitometric quantitation after Phosphorimaging using Multigauge V3.2 software (Fuji). Lane tracings were made by ImageQuant 5.1 software (GE Healthcare). Each experiment was performed at least three times and all gel data shown represent that which was reproducible.

RESULTS

3 bp of rU:dA hybrid and 5T on the NT strand is a minimal terminator for RNAP III

Studies of *S. cerevisiae* (sc) RNAP III ECs established that while RNAP III-core terminates in the distal part of a

9T terminator at positions 8–9, RNAP III-holo terminates more proximally (34,35). Sequence identity at oligo(dT) positions 3–5 of the NT DNA was established as important for termination, but impact of the rU:dA hybrid was not systematically examined (35). To better define *cis* elements involved, we began with a 5T-5A terminator because this is the minimum T length required for functional, albeit less than highest efficiency termination in yeast (41,42). We analyzed RNAP III ECs on scaffolds with substitutions limited to the TZ of either the NT or the T DNA strands as in Figure 1A. A ^{32}P-5′ end labeled 10 nt RNA is annealed to the DNA T strand to which immobilized RNAP III is added. The NT DNA strand is then added and annealed followed by washing and addition of NTPs. The 10-min transcription reaction is separated into supernatant, representing the terminated or released (R) RNA fraction, and the bound (B) RNA fraction that remains associated with RNAP III; immediately upon separation each fraction is mixed with phenol to stop the reaction. Lanes 1 and 2 of Figure 1B show the R and B products; termination is revealed by RNA released mostly at positions 3, 4 and 5 in the TZ. Reducing the number of As on the T DNA strand from 4 to 3 resulted in a downward shift in RNA size, to a majority at position 3 although the total amount of RNA was generally maintained (Figure 1B, lanes 1, 3, 5). Limiting the number of As on the T DNA strand to two inhibited termination as seen by the ratio of RNA in TZ versus RT region of lane 7 versus lanes 5, 3 and 1 of Figure 1B, as well as these RNAs in lanes 8, 6, 4 and 2.

A contiguous stretch of 5T on the NT strand supports efficient termination whether there is 5 or 3 As on the T strand (Figure 1C, lanes 1–4). 5T with 3A in the T strand supports termination whereas 4T with 3A does not (Figure 1D, lanes 5–6 versus 11–12). Requirement for 5T is not explained by lack of base pairing at the distal end of the tract (Figure 1D, compare lanes 5–6 with 7–8). Thus, 5T-3A is a minimal terminator for RNAP III for mechanistic studies.

Termination by RNAP III holo and core differ in sensitivity to the rU:dA hybrid

We compared termination efficiency (TE) by RNAP III-core and -holo at 5T-5A and 5T-3A terminators (Figure 2A). Holo TE was ∼50% at both terminators (lanes 1–4). Although TE for core was lower than holo at 5T-5A as expected, in contrast to holo, core TE at 5T-3A was markedly reduced relative to TE at 5T-5A (8 versus 23%; lanes 5–8). Note that while TE accounts for both R and B RNAs, the ratio of TZ to RT RNAs in the same lane, R, is an internally controlled, independent reflection of termination efficacy. The single lane analysis can also be applied to the B fractions, as in lanes 2, 4, 6 and 8 of Figure 2A which shows that core is much more deficient than holo at 5T-3A than at 5T-5A.

The existing model to explain C37/53 action in termination is that it decreases elongation rate and promotes termination via kinetic coupling (10). Figure 2A suggests that sensing rU:dA hybrid strength/length may be a novel termination activity of C37/53/C11 distinct from effects on elongation rate and that these effects may be distinguishable. It was shown that TE by RNAP III-core at a 7T terminator increased as UTP concentration decreased, consistent with the kinetic coupling model (10). We examined TE by RNAP III-holo and core as a function of decreasing NTP concentration on scaffolds that differ in RNA:DNA hybrid strength due to oligo(rU:dA) length. Here we compared 6T-6A and 6T-3A terminators (Figure 2B and C; Supplementary Figure S2), although comparable outcomes were obtained comparing 5T-5A and 5T-3A (not shown). The TE of RNAP III-core increased sharply at 6T-6A as NTP concentration decreased (Figure 2B), achieving ∼90% at 5 uM NTP, consistent with previous data observed upon decreasing UTP only (10). At 6T-3A the TE of holo increased sharply to ∼90% at 5 uM NTP (Figure 2C). However, by contrast to its behavior at 6T-6A, RNAP III-core neither sharply increased nor achieved high TE at the lowest NTP concentration when limited to the 3 bp rU:dA hybrid terminator, 6T-3A (Figure 2C). These data support the idea that RNAP III-holo and RNAP III-core differ in TE in a way that cannot be accounted for by kinetic coupling alone and that differential sensitivity to rU:dA hybrid strength is likely a distinct component.

A weak RNA:DNA hybrid can compensate for lack of C37/53/C11 in termination

The RNA:DNA duplex upstream of an oligo(rU:dA) terminator can contribute to the overall strength of the hybrid in the active center binding site. To examine effects of this on RNAP III-holo and core, we systematically increased the %G+C content 5 bp upstream of the rU:dA stretch (Figure 2D). This had progressive negative effects on TE by RNAP III-core but negligible effects on holo (Figure 2D). Although other possibilities exist, these data support the idea that RNAP III-core exhibits innate propensity for autonomous termination at RNA:DNA hybrids of low thermal stability and that a long stretch of rU:dA is required to manifest this (e.g., the 9T:9A terminator in the absence of C53/37) (34).

Weakening the rU:dA hybrid with 4sU can compensate for lack of C37/53/C11

The universal mechanism of NTP selection for catalysis during RNA synthesis is conserved among RNAPs I, II and III (43,44). A single binding site accommodates the pyrimidine and purine NTPs and some analogs thereof, and selection of the cognate base depends on Watson:Crick hydrogen bonds with the DNA template strand nucleotide which positions it in the active site (43).

The uridine-triphosphate analog, 4-thio-UTP (sU) is used for incorporation into RNA in place of UTP to study RNA synthesis and/or decay rates *in vivo* (45,46). Yeast RNAP II can use UTP and sUTP with very similar kinetics; the slight difference in K_M (which is in the low nM range) was attributed to weaker base pairing between 4sUTP and the template, as based on modeling into the active site of the crystal structure of a RNAP II EC (45). The weak base pairing characteristic of sU had previously been used to examine effects of decreased RNA:DNA hybrid stability on elongation arrest after its incorporation into the RNA by *Escherichia coli* RNAP (47).

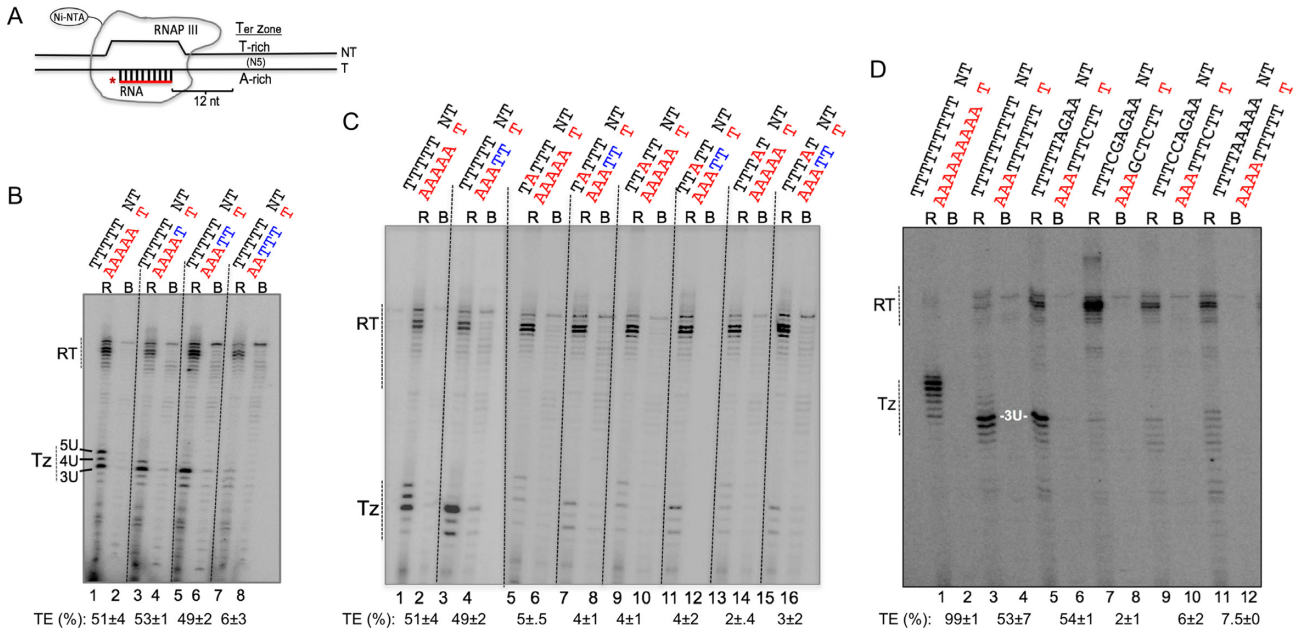

Figure 1. Definition of a RNAP III minimal terminator for mechanistic study. (**A**) Schematic of RNAP III EC assembled on oligonucleotide scaffold. The first T:A bp of the TZ is 12 bp downstream of the 3′ end of the 10 nt RNA primer; red asterisk indicates 5′-^{32}P. The numbers of Ts and As in the NT and T strands respectively vary in panels **B**–**D** as indicated above the lanes. (B) Gel autoradiogram showing 10 min transcription assay with T5 on NT strand and A2, A3, A4 or A5 on T strand as indicated. Transcripts released from, and bound to immobilized RNAP III are indicated above the lanes as R and B, respectively. Tz denotes the TZ positions and RT denotes read through. (C and D) Transcriptions as in panel B with the NT and T sequences indicated above the lanes. Quantification of TE is shown below the lanes with S.D. triplicate experiments. Each experiment was performed at least three times and the data shown represent that which was very reproducible.

We asked if weakening the rU:dA component of the hybrid by substitution of UTP with sUTP in transcription reactions might increase TE and also compensate for lack of C37/53/C11. For this we employed the 5T-5A terminator preceded by the 80% G+C upstream region used in Figure 2D. RNAP III-holo released RNAs that were shorter after incorporating sU than after incorporating U, and TE also increased (Figure 2E, lanes 1–2 versus 3–4). Importantly, TE increase with sU was more striking for RNAP III-core; while it was low on the 80% G+C upstream terminator with U, it was increased several-fold with sU (Figure 2E, lanes 5–6 versus 7–8). The TE achieved with (rsU:dA) by core was comparable to that achieved with (rU:dA) by holo (Figure 2E, 59% versus 53%; lanes 7–8 versus 1–2). We also noted more arrest with core than with holo as reflected by a significant proportion of transcripts bound to the polymerase (Figure 2E, lane 8, see below). Thus, multiple approaches and biochemical evidence indicate that weakening the RNA:DNA hybrid can compensate for lack of C37/53/C11 in termination. The data support the conclusion that C37/53/11 serves to sensitize RNAP III to the RNA:DNA/rU:dA hybrid and thereby promote termination in oligo(T) tracts.

C11 reconstitutes/stimulates termination independent of its RNA 3′ cleavage activity

If the termination deficiency of RNAP-core relative to RNAP-holo on the 5T-3A minimal terminator is due to absence of C37/53, it should be reconstituted/rescued by addition of recombinant C37/53 and C11. In previous studies that employed relatively efficient terminators, C37/53 added to RNAP III-core could restore the pattern of terminated transcripts to that more similar to RNAP III-holo and this was slightly enhanced by C11 (34,35). Here, use of the minimal terminator revealed more substantial effects (Figure 2F). RNAP III-holo produced ∼50% TE on the 5T-3A terminator, whereas TE by core was ∼8% (Figure 2A, lanes 3, and 7, and Figure 2F, lanes 1 and 3). Addition to core of C11 that is either wild-type (WT) or mutated at D91A, E92A (C11^{AA}, C11-M) to inactivate its RNA 3′ cleavage activity, had negligible effect on TE (Figure 2F, lanes 5–8). Addition of C37/53 to core significantly increased TE from 8-9% to ∼15% (Figure 2F, lanes 3, 5, 7 vs. 9). Addition of C37/53 together with C11-WT or C11-M increased TE to ∼45%, substantially higher than with either protein alone (Figure 2F, lanes 11–14) and comparable to RNAP-holo. That this C11-M is inactive for RNA 3′ cleavage activity will be shown in a later section. Thus, C37/53/11 can reconstitute the TE deficiency of RNAP-core on the minimal terminator. In addition, this data provide evidence that C11 stimulates C37-53-dependent termination in a defined *in vitro* system, and moreover, that it does so in a manner that is independent of its RNA cleavage activity.

Sensitivity of RNAP III-core to proximal terminator arrest after incorporation of sU

When sU was used on the 9T terminator, RNAP III-holo released short RNAs as compared to with U (Figure 3A, lanes 1–4). This supports the idea that the holoenzyme re-

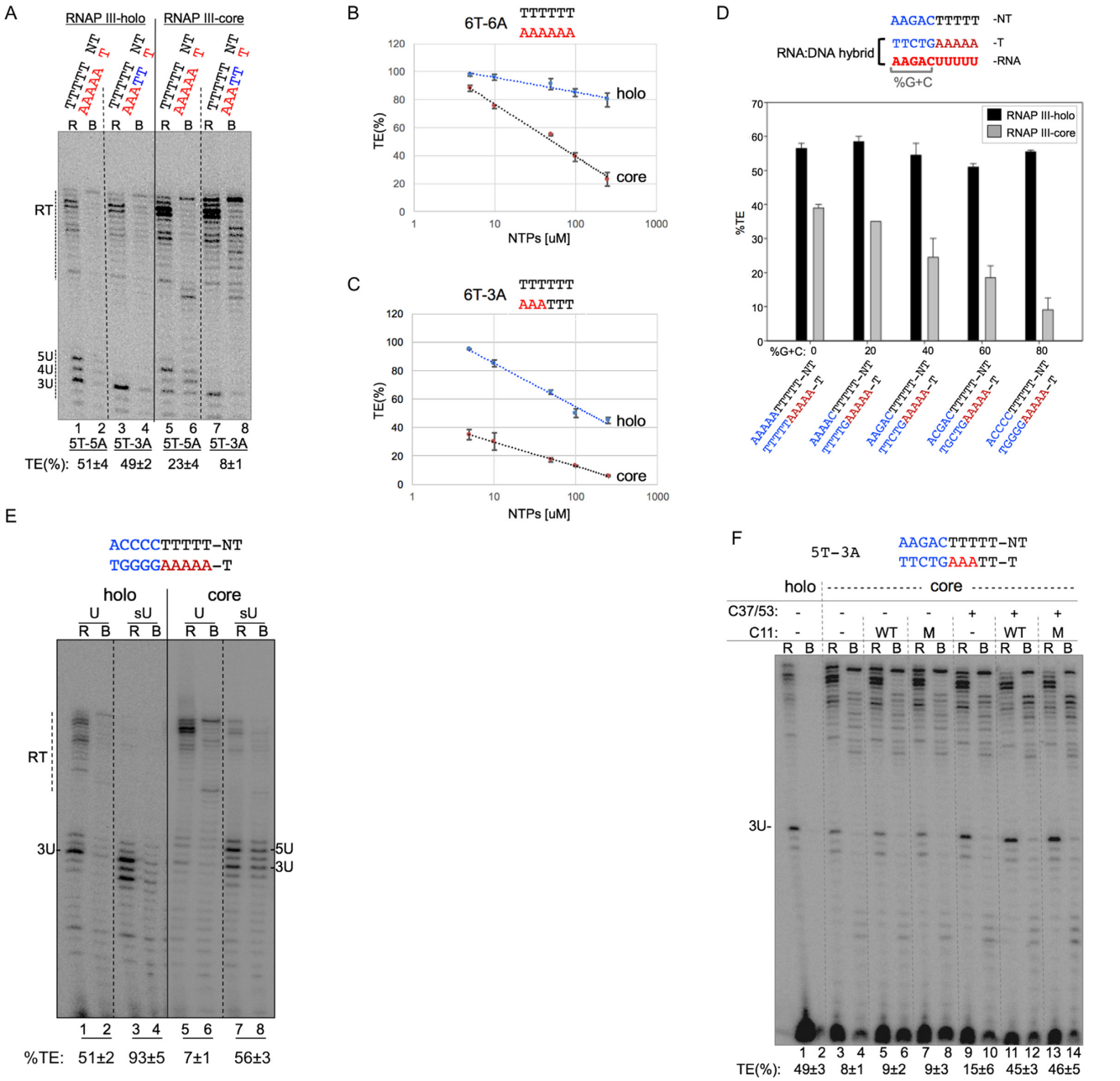

Figure 2. RNAP III-core is deficient in sensitivity to the RNA:DNA terminator hybrid and can be complemented by C37/53 and C11. (**A**) Transcription using RNAP III-holo and -core on the 5T-5A and 5T-3A terminator scaffolds. TE (%) was calculated as in 'Experimental procedures'. Numbers represent two experiments ±SE. (**B** and **C**) TE versus NTP concentration for RNAP III-holo and -core on 6T-6A and 6T-3A terminator scaffolds, respectively; error bars reflect duplicate experiments. (**D**) Top shows schematic depicting 5 bp varied in %G+C content upstream of 5T-5A terminators for the TE data in the graph; these terminators differ in potential strength of upstream part of RNA:DNA terminator hybrid as plotted on *X*-axis. Error bars reflect standard error of two experiments. (**E**) Transcription by RNAP III-holo and core as in (A) but using the 80%G+C upstream-5T-5A terminator from (D) and NTPs containing sUTP or UTP as indicated. (**F**) Termination at the minimal terminator, 5T-3A by RNAP III-holo (lanes 1–2), and RNAP III-core (lanes 3–14) complemented by the components indicated above the lanes. The C11 subunit is either WT or the mutated version (M, $C11^{AA}$).

sponds to RNA:DNA hybrid destabilization in the proximal T tract by terminating transcription. RNAs produced by RNAP III-core were also shorter with sU as compared to U, although in striking contrast to holo, a large fraction of RNAP-core arrested in the proximal T tract rather than continue to elongate or release (Figure 3A, lanes 7–8).

It is important to note that the propensity for RNAP III-core to arrest in the 9T terminator was noted previously using UTP (see Figures 2C and 5C in ref (34)). 4sU appears to greatly exacerbate this propensity and may therefore provide insight into the mechanism of this arrest. This propensity doesn't necessarily fit with the overall faster elongation rate of core relative to holo (9) and suggest that C37/53 and C11 contribute to termination by a mechanism(s) more complex than previously thought.

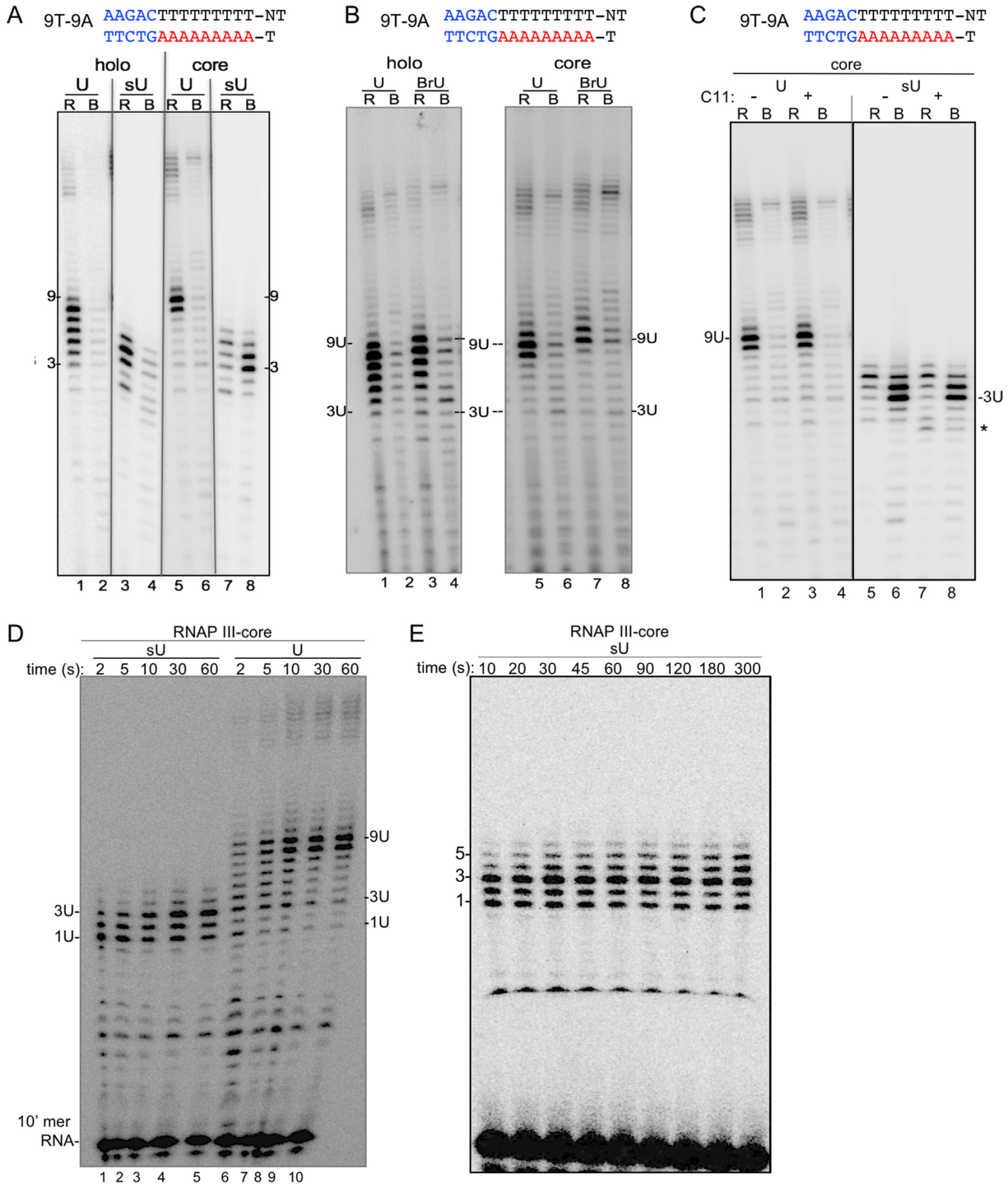

Figure 3. A weak rU:dA terminator hybrid arrests RNAP III-core with RNA 3′ end displacement. (**A**) Ten minute transcription reaction with ATP, CTP, GTP and either sUTP or UTP on the 9T-9A terminator scaffold by RNAP III-holo and -core. (**B**) As in A but using 5-BrUTP in place of UTP as indicated above the gels. (**C**) Transcription by RNAP III-core on the 9T terminator scaffold with A, G, C and either U or sU in the presence of C11 as indicated. The asterisk indicates sU-specific products of C11. (**D**) Early time courses of transcription on the 9T-9A terminator scaffold by RNAP III-core as in A but from 2 to 60 s comparing sUTP and UTP. (**E**) Time course of transcription on the 9T-9A terminator scaffold by RNAP III-core from 10 to 300 s with ATP, CTP, GTP and sUTP.

The cumulative data suggest that proximal arrest in the 9T tract may be due to some type of misposition of the RNA:DNA hybrid in the active center of RNAP III-core as a result of the weakening effects of sequential 4sUs in the rU:dA hybrid. Alternatively, the observed arrest might be due to a general bulkiness of the sU analog, which might affect activity of the polymerase active center. Insight into these alternative interpretations may benefit from incorporation of another uridine-triphosphate analog, 5-bromo-U (BrUTP), which exhibits increased strength of Watson:Crick base pairing, is more massive and bulky than sU, and has been widely used for RNA metabolic labeling (46,48), as well as for studying the effects of altering the stability of the RNA:DNA hybrid on RNA polymerase elongation (47). In addition, BrU incorporation would also allow potential observation of effects of strengthening the rU:dA hybrid. First and most importantly, in contrast to sU, which caused >60% arrest in the proximal part of the 9T terminator after a 10 min transcription reaction (Figure 3A, lanes 7–8), replacement of U with BrU did not cause significant arrest by RNAP III-core in the 9T terminator (Figure 3B, lanes 7–8). Second, incorporation of BrU shifted termination downstream as compared to U; for RNAP III-holo the effect was subtle but evident in the ratio of the 8:9 positions (Figure 3B, lanes 1 and 3; also note slight up-shift in mobility as number of heavy BrUs accumulate in the RNA chain). However, the effect of BrU on RNAP III-core was somewhat more dramatic with greater distal traverse of the 9T terminator than with U again evident in the ratio of the 8:9 positions (Figure 3B, compare lanes 5 and 7). Arrest by RNAP III-core after incorporation of sequential 4sUMP residues in the 9T terminator could not be prevented by inclusion of C11 in the transcription reaction (34,35). While C11 did show some evidence of RNA cleavage in the sU containing transcription reaction (Figure 3C, asterisk), it did not prevent proximal arrest of RNAP III-core by sU incorporation (Figure 3C).

In summary, the most profound results obtained with the U analogs was that oligo(sU) led to arrest in the proximal region of the 9T terminator. As will be supported by data below, this is most likely due to a weakened RNA:DNA hybrid.

In 10 min transcription reactions, RNAP III-core became arrested after incorporating sU residues with near equal distribution at positions 3 and 4 in the 9T tract (Figure 3A, lane 8). Because RNAP III normally traverses the proximal part of the 9T terminator in a few seconds (35) and RNAP III-core is generally faster than holo (9), we hypothesized that the apparent arrest is due to the destabilized (rsU:dA) hybrid and displacement of the sU 3′ end by melting away (fraying) from the template DNA strand active site. Accordingly, by breathing of the rU and dT strands the sU 3′ end would only transiently engage the active site, limiting the time during which an incoming sUTP could promote extension. The data in Figs 3D and E described below are consistent with this hypothesis.

We examined the kinetics of sU incorporation as compared to U as a time course of transcription from 2 to 60 s on the 9T terminator scaffold (Figure 3D). This showed that sU incorporation distributed to the first three positions by 10 s then accumulated mostly at position 3 thereafter, whereas U distributed through all 9 positions at 2 and 5 s and accumulated at the 8 and 9 positions predominantly by 10 s, similar to previous results (35). A 5-fold longer time course, up to 300 s showed that position 3 is indeed a major impediment to extension in the presence of sU as elongation beyond this was very slow (Figure 3E) consistent with the data in Figure 3A and C.

Evidence for fraying of the RNA 3′ end of a weakened RNA:DNA hybrid

It is known that a cause of transcription arrest is due to detachment of the RNA 3′ end from the active site, and that this can be due to weakening or destabilization of the RNA:DNA hybrid (47). Accordingly, the data in Figures 2E and 3A would suggest that RNAP III-core has greater propensity than RNAP III-holo for RNA 3′ end detachment as the hybrid is weakened by increasing oligo(sU) length. According to this model of RNAP III arrest by sU incorporation, the RNA 3′ end would detach by fraying rather than extrusion from the catalytic site as would occur by backtracking (backward translocation) of the polymerase. This may resemble the elemental pause state of bacterial RNAP which contains a frayed RNA 3′ end nucleotide that can inhibit further nucleotide addition without backtracking (49,see 50) or a RNAP II EC with a RNA 3′ frayed end that blocks the incoming NTP site and halts transcription (51), although these RNAP III-core sU-arrested complexes are likely unique. In Figure 4 we used approaches to assess potential fraying of the RNA 3′ end after incorporation of three or more sequential sU nucleosides by RNAP III-core. In Figure 4A and B we examined the relative sensitivities of artificially stalled RNAP III-core ECs, after incorporation of 4U or 4sU, to the RNA 3′ cleavage subunit, C11. After stalling on a C-free cassette in the absence of CTP, the ECs were isolated and washed extensively before C11 was added and left to incubate for the times indicated (Figure 4A). It is noteworthy that the scaffold used here does not contain a 5T tract on the NT DNA strand and would not comprise an efficient functional terminator. This and similar analyses revealed that while the ECs that were stalled after UMP incorporation were relatively resistant to cleavage by C11 over the 15 minute time course (Figure 4A, lanes 1–4), the ECs stalled after sUMP incorporation were relatively sensitive (lanes 5–8). This was apparent by appearance of bands corresponding to positions 1sU and G-1 in the predicted transcription bubble region in the sU reaction, as well as the G-10 band. Note that G-1 and G-10 reflect RNA ends after cleavage of sU residues immediately adjacent to 1U and -9U (see schematic at top of Figure 4A). Figure 4B shows the lane tracings of the gel in Figure 4A; UMP upper panel, sUMP lower panel.

A RNAP III-core pre-termination complex in an arrested state

We hypothesized that RNAP III-core complexes that arrested in the proximal part of the 9T terminator after 3 min of sU incorporation in the presence of the other three NTPs as in Figure 3E, could be isolated, washed free of NTPs and then subjected to a second elongation reaction with regular UTP. This would allow extension if the RNA 3′ sU end

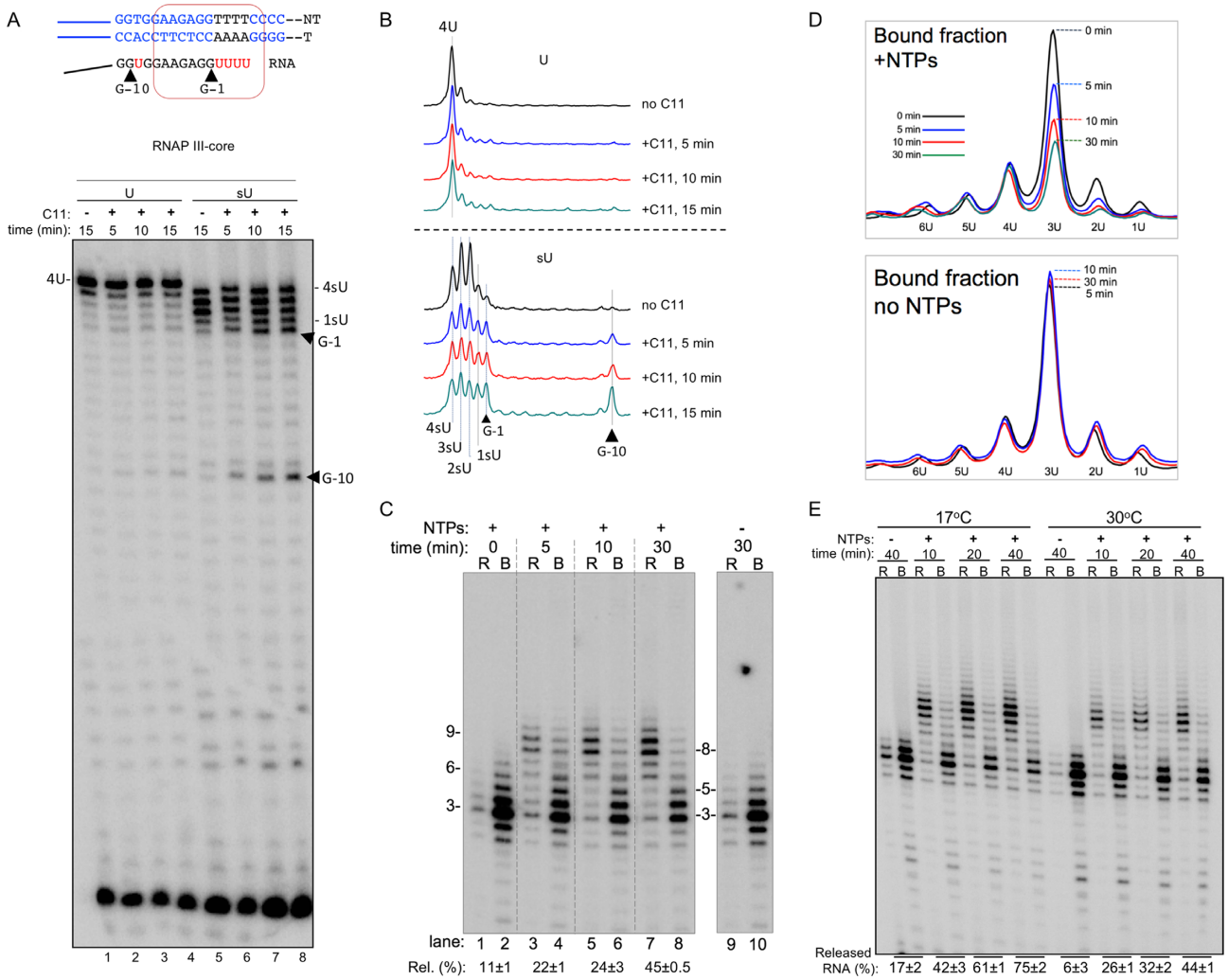

Figure 4. Evidence for RNA 3′ end fraying after sU incorporation by RNAP III-core. (**A**) Comparison of sensitivity to RNA cleavage by C11 of stalled transcription ECs (not a pre-termination complex; see text) after incorporation of four U residues or four sU residues. Top shows schematic of distal end of C-free cassette template (and NT) strands, and schematized 39-mer RNA produced with ATP, GTP and either UTP (lanes 1–4) or sUTP (lanes 5–8) in autoradiogram below. The positions of G at −1 and −10, relative to the U4 tract are indicated by filled triangles. After transcription elongation by RNAP III-core in the absence of C11, stalled complexes were isolated and washed three times before C11 was added and incubated for the times indicated above the lanes. (**B**) Lane tracings of the gel in A (see text). (**C**) After a 5 min transcription reaction in the presence of 100 uM NTPs (A, G C and sU), the sU-arrested RNAP III-core complexes were isolated and washed, and used to examine the time course of elongation in a second reaction containing NTPs containing UTP instead of sUTP. (**D**) Lane tracings of the bound fractions of panel C in the presence of NTPs (top) and absence of NTPs (bottom). (**E**) Transcription of isolated sU-arrested RNAP III-core complexes in a second reaction containing NTPs with UTP instead of sUTP at 17°C and 30°C as indicated. Quantitation of RNA extended and released is shown under the lanes as standard error (SE) from duplicate experiments.

was frayed and could transiently re-engage the active site. We hypothesized that re-engagement would be slow and dependent on position; the farther extended the RNA-sU was in the original arrested complex the more destabilized the hybrid would be and the more the 3′ end would be frayed from the template in the active site and refractory to extension by regular UTP. According to this model, incorporation of regular UMP would stabilize the RNA 3′ end, promote elongation, and the oligo(U)-extended RNA would be terminated farther in the distal part of the 9T tract. Therefore, we isolated and washed the immobilized sU-arrested RNAP III-core complexes and then subjected them to a time course exposure to four NTPs containing regular UTP (Figure 4C). As expected, the sU-arrested complexes were not irreversibly arrested as their RNA was extended by UTP and terminated, albeit at a remarkably slow rate (Figure 4C, lanes 1-8, compare with Figure 3D, lanes 6–10), as expected. Lanes 9–10 show that the isolated complexes were stable over the 30 min course in the absence of NTPs. These data are consistent with the RNA 3′ end fraying model.

Notably, positions 2 and 3 of the sU-arrested RNAP III-core complexes were preferentially depleted from the arrested (B fractions) relative to positions 4 and 5 as the reaction proceeded (Figure 4C) as graphically represented in the top panel of Figure 4D which shows quantitative tracings of lanes 2, 4, 6, 8 of Figure 4C. Such preference would be expected if position 4 complexes were more refractory to elongation than position 3, i.e. because four consecu-

tive sU residues would destabilize the oligo(rsU:dA) hybrid more so than three sU residues, and this would cause greater RNA-sU-3′ end displacement/melting. By contrast, relative amounts of all positions were stable over time in reactions lacking NTPs (Figure 4D, bottom panel). This pattern would not as readily be explained by a model in which the sU-arrested complexes were reactivated by active site mediated cleavage.

A prediction of the model in which incorporation of sequential sUMP residues weakens the rU:dA hybrid to the point of RNA 3′ end fraying is that decreasing temperature would favor hybrid stabilization by RNA 3' end annealing with the template and increase the rate of subsequent UMP incorporation. Figure 4E showed this to be the case. By decreasing the temperature to 17°C, ∼75% of the sU-arrested complexes were reactivated by NTPs with UTP after 40 minutes whereas this was ∼44% at 30°C (Figure 4E).

The data support a model in which the RNAP-core enzyme becomes progressively susceptible to arrest in the 9T tract after incorporation of sequential sUs in a length-dependent manner because the RNA 3′ end becomes disengaged from the active site with increasing destabilization of the rU:dA hybrid. The arrested state is reversible because the RNA-sU 3′ ends can transiently base pair with the template in the active site and be elongated by UMP in the subsequent extension reaction.

We examined the sU-arrested complexes after incubation with four NTPs, UTP only, or ACG, in 5 min. reactions (Supplementary Figure S3). UTP promoted elongation and termination in the distal 9T terminator as expected of RNAP III-core as did all four NTPs, whereas AGC lacking UTP failed to rescue arrest or promote elongation (Supplementary Figure S3).

The above kinetic analyses and other data provide evidence that the propensity of RNAP III-core to arrest after incorporation of sequential 4sUMPs is due to transient melting of the RNA 3′ end from the template and associated disengagement from the active site.

C37/53 promotes RNA 3′ end active site engagement in the proximal terminator

RNAP III-holo terminates more proximally in the 9T terminator than does RNAP III-core (34) (Figure 3A, lanes 1 and 5). Also, a significant fraction of RNAP III-core arrests in the 9T terminator after UMP incorporation (34) and exhibits much more propensity to arrest after sU incorporation as compared to RNAP III-holo and this is not prevented by supplementing the core enzyme with excess C11 (Figure 3C), suggesting that C37/53 prevents this arrest (Figure 2E, lanes 7–8, Figure 3A, lanes 7–8). We therefore examined C37/53 for potential reversibility of isolated RNAP III-core sU-arrested complexes (as assayed as in Figure 4C). Addition of C37/53 and NTPs to isolated RNAP III-core sU-arrested complexes had two effects, a proximal shift in termination (Figure 5A) and an increased rate of arrest reversibility (Figure 5B), the latter presumably by promoting RNA 3′ engagement. Reconstitution with C37/53 prior to NTP addition (Figure 5A, lanes 9–16) led to a proximal shift in termination with RNAs released at positions 6, 8 and 9 (lanes 11, 13, 15), whereas in the absence of C37/53, RNAs were released more distally, predominantly at positions 8 and 9 (lanes 3, 5, 7). Position 6 clearly reflects proximal termination, a characteristic of RNAP III-holo (compare lanes 1 and 5 of Figure 3A). Note also that some position 5 RNA increases in the released fraction over time in the presence of C37/53 but not in its absence (Figure 5A, compare lanes 15 and 7). Notably, these data provide evidence that the proximal termination pattern of position 6 RNA observed here with C37/53, and with RNAP III-holo, does not require C11-mediated cleavage of longer RNAs.

We quantified the percentage of sU-arrested RNA that was extended and released from the RNAP III-core complexes after NTP addition in the presence and absence of C37/53 over time (Figure 5B). The analysis showed that C37/53 increased the efficacy with which the sU-arrested RNA was extended (Figure 5B). This provides evidence that the C37/53 heterodimer promotes engagement of the RNA 3′ end with the active site. We refer to the ability of C37/53 to promote RNA 3' end engagement in the proximal part of an oligo(T) tract and further extend the RNA to a productive termination product as catch and release.

The C37 CTD termination-initiation loop and C53-NTD promote optimal activity

It was previously shown that a C37/53 heterodimer containing a mutant C37 deleted of residues 226–230 disables transcript release after the proximal pause in the 9T terminator (35). Here we used a C37*/53 heterodimer that contains five alanine substitutions in positions 226–230 of the C37-CTD in 30 min. transcription reactions on isolated RNAP III-core sU-arrested complexes (Figure 6A). Addition of C37/53 without NTPs reproducibly increased RNA release, quantified as TE from duplicate experiments shown under lanes 5–6 versus 1–2 of Figure 6A. C37/53 +NTPs again led to high TE with the distinctive feature of proximal termination reflected by position 6 and 5 RNAs in the R fraction (Figure 6A and B, compare lanes 7 and 3). The C37*/53 heterodimer was deficient for proximal termination relative to WT C37/53 (Figure 6A and B, compare quantitative lane tracings (black, released) at positions 7, 6 and 5 for lanes 7 and 11). Additional deficiency of C37*/53 was reversal of position 3 arrest in +NTPs (Figure 6A compare lanes 8 and 12, Figure 6B, blue lane tracings).

It was shown that the C37/53 heterodimer lacking the first 279 amino acids of C53 but retains its dimerization domain was specifically deficient in preventing arrest by RNAP III-core in the 9T terminator with UTP (34,35) The same mutant C37/53* heterodimer was deficient for termination at positions 6 and 5 relative to WT C37/53 in the reactions in (Figure 6A and B, compare quantitative lane tracings (black, released) at positions 5–7, lanes 7 versus 15). This mutant heterodimer was also deficient in reversal of position 3 arrest in +NTPs (Figure 6A compare lanes 8 and 16, Figure 6B, blue lane tracings). These data from each of both subunit mutants suggest that ability of C37/53 to reverse arrest in the early part of the T tract (position 3) may be related to its ability to promote RNA release in the proximal terminator at positions 5 and 6 (below).

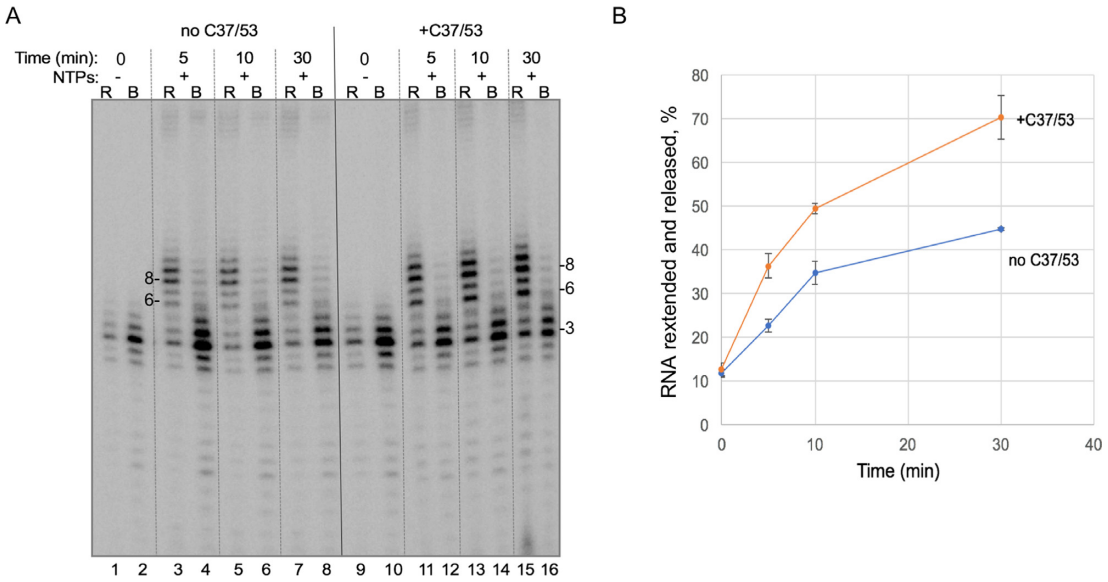

Figure 5. C37/53 promotes RNA 3′ end elongation activity from sU-arrested complexes. (**A**) Time course of transcription of isolated sU-arrested RNAP III-core complexes in the absence and presence of C37/53. (**B**) Quantification of the % RNA extended and released from analysis as in panel A; error bars reflect standard error (SE = Standard deviation/$\sqrt{n}$). The standard deviations are as follows: 2.5, 4.7, 2.1 and 8.5 for 0, 10, 20 and 30 min, respectively, without C37/53 and 1.5, 2.5, 4.5 and 0.58 for 0, 10, 20 and 30 min, respectively, with C37/53.

C37/53 can promote termination in the absence of NTPs, elongation or C11

For the assay used in Figure 6A and others above, transcription with sUTP in place of UTP generates arrested complexes that are isolated and washed four times with buffer containing no NTPs prior to addition of buffer and recombinant proteins, incubation and separation into R and B fractions ('Materials and Methods' section). We surprisingly observed that C37/53 reproducibly terminated position 3 RNA in the absence of NTPs (Figure 6A, compare TE, lanes 5–6 versus 1–2) using a standard method for determining TE (52,53). This novel observation suggests that RNA release may be limited to when the RNA 3′ end is in the active site of the RNAP III termination complex. Therefore, it was important to document further reproducibility and also use another method to quantify the R and B fractions (54,55), which we refer to as TE_Q (Figure 6C). This method is thought to be less susceptible to potential pipetting error as compared to standard TE as quantitation is derived from half of the R fraction in one lane (R) and a mix of 1/2R plus the B fraction in another lane (R+B) for each reaction sample (54,55) (Methods). Thus, the assay on RNAP III-core sU-arrested complexes was performed and quantified this way (Figure 6C). TE_Q in Figure 6C indicate that C37/53 terminated the position 3 sU RNA in the absence of NTPs whereas C37*/53 and C37/53* were each significantly impaired. As a control for these reactions, the arrested complexes were incubated with C37/53 and mutant heterodimers in the presence of NTPs (Figure 6C, lanes 9–16). This showed a higher activity of C37/53 for extension to proximal termination as compared to the mutant heterodimers (compare lanes 11, 13, 15), and depletion of position 3 RNA.

That C37/53 stimulates release in the absence of NTPs, led us to hypothesize that if release/termination is limited to when the RNA 3′ end is in the active site, this reaction may also be limited by transient access due to hybrid RNA 3' end breathing and exhibit kinetics similar to extension by NTPs containing UTP. RNA release from the sU-arrested complexes in the absence of NTPs was indeed very slow and C37/53 increased its efficacy (Figure 6D and E). The data are consistent with the idea that a shared step, transient engagement of a frayed RNA sU-3′ end with the active site, limits RNA release in the absence of NTPs and RNA extension in the presence of NTPs, and that C37/53 promotes this step. Moreover, the data provide evidence to suggest that for RNAP III, an RNA 3′ end in the active site is a determinant of termination.

C37/53 can temper the active site RNA 3′ cleavage activity stimulated by C11

Data above indicate that C37/53 promotes RNA 3′ end engagement with the active site in a manner and by a mechanism that doesn't benefit from C11. Figure 4A showed that C11 could cleave 3′ sU-RNA from RNAP III-core that was artificially stalled on a 4T non-terminator complex. Next we examined interplay between C11 and C37/53 activities on sU-arrested complexes on the 9T pre-termination complex. Figure 7A shows that C11 added to isolated sU-arrested complexes in the absence of NTPs produced cleavage products as expected (lane 4). However, with C37/53 present together with C11, a significant amount of position 3 RNA was released and the cleavage products were decreased (lanes 5 and 6). The band patterns would suggest that C37/53 competed with C11 for the position 3 RNA and diverted it to the termination pathway.

C11 exhibits robust RNA 3′ cleavage activity on RNAP III-core complexes that are in a backtracked state due to assembly with a 3′ overhang of 2 mismatched nts, as depicted in Figure 7B (34). The Figure 7B gel shows that C11-

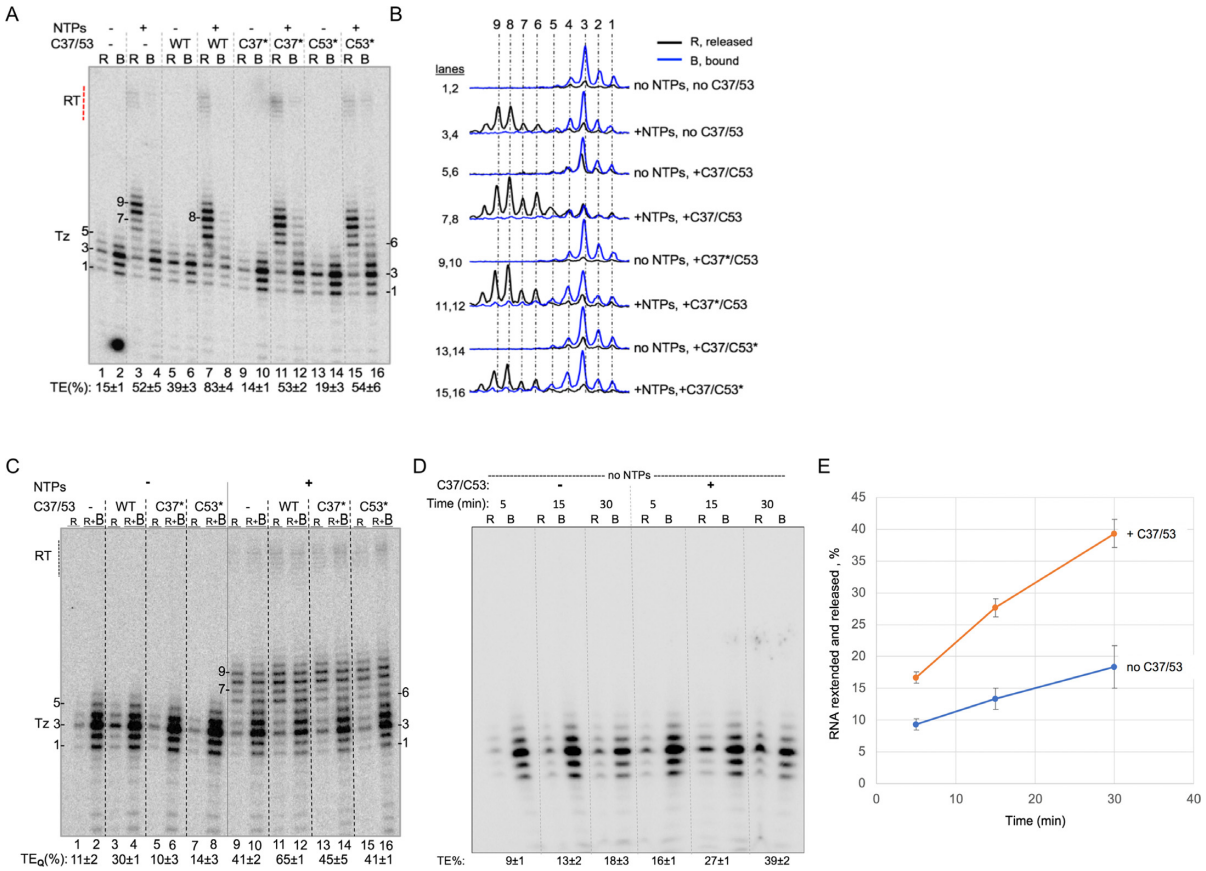

Figure 6. C37/53 domains involved in terminator RNA 3′ end catch and release activity. (**A**) Isolated sU-arrested RNAP III-core complexes on a 9T-9A terminator were washed and incubated with buffer alone (lanes 1–2) or with components indicated above the lanes for 30 min, stopped and separated into R and B fractions. TE is indicated below the lanes based on duplicate experiments. (**B**) Quantitative tracings of the lanes of the gel shown in A. (**C**) Same as panel A but analyzed for quantitation in triplicate by the half-supernatant/half supernatant+bound method (54,55), in the absence of NTPs (lanes 1–8) and presence of NTPs with UTP (lanes 9–16). $TE_Q = (2R)/[(R) + (R+B)]$ x 100. Note that the R lanes contain half of the supernatant material and R+B lanes contain half of the supernatant *plus* the bound material. (**D**) Time course of RNA release (termination) from isolated sU-arrested RNAP III-core complexes in the absence of NTPs, in the presence and absence of C37/53. (**E**) Quantification of the % RNA released from analysis as in panel D; error bars reflect S.E. derived from duplicate experiments.

stimulated RNA cleavage is inactivated by the $C11^{AA}$ mutations (C11-M) (compare lanes 4 and 6); note that total RNA was analyzed without separation of R and B fractions. RNA bands representing cleavage of the overhang in lane 4 were more intense than the lower bands suggesting that C11 exhibits greater activity for the overhang than for the intrinsic RNA 3′ end that is positioned in the active site (see cartoon above 7B gel). The relative amount of cleavage of the 2 nt overhang was similar in the presence and absence of C37/53, whereas products of intrinsic cleavage were differentially inhibited by C37/53 (Figure 7B, lane 8 versus 4).

These data argue that C37/53 can modulate C11-stimulated intrinsic RNA cleavage. The data support a role for C37/53 in maintaining the RNA 3′ end in register with the active site, and further, that C37/53 can protect the RNA 3′ end from C11-mediated cleavage stimulation.

Recombinant C37/53 plus C11 partially rescue sU-mediated arrest by RNAP III-core

To gain insight into the mechanism of sU-mediated arrest, we examined if ECs reconstituted with RNAP III-core plus recombinant C37/53 and/or C11 could prevent arrest after extension with sUTP, CTP, ATP and GTP using the 9T terminator scaffold (Figure 8A and B). With sUTP present in place of UTP, RNAP III-holo led to ∼85% TE (∼15% arrest), whereas TE (release) by RNAP III-core was only ∼13.5% (∼86.5% arrest, Figure 8A, lanes 1–4). Reconstitution with C11 prior to addition of sU/C/A/GTP had little effect on the formation of sU-arrested transcripts (Figure 8A, lane 6) but produced released RNA at position −1 (*) with an increase in TE from 13.5 to 25.3% (lanes 3–6). Addition of C37/53 increased TE to 34.2% with released RNAs at positions 5 and 1 but not −1 (Figure 8A and B, lane 7). Addition of C37/53+C11 yielded 51% TE (49% arrest), including released RNA at -1 yet this was still substantially lower than achieved with RNAP III-holo and the RNA distribution patterns were also dissimilar (compare lanes 1 and 2 with 9 and 10) (‘Discussion’ section).

In summary, Figure 8A shows that while C37/53 alone does not prevent arrest it decreases it by promoting further elongation and termination farther in the 9T terminator (lanes 7 and 8). However, the combination of C37/53 and C11 has a larger effect on preventing arrest, decreasing

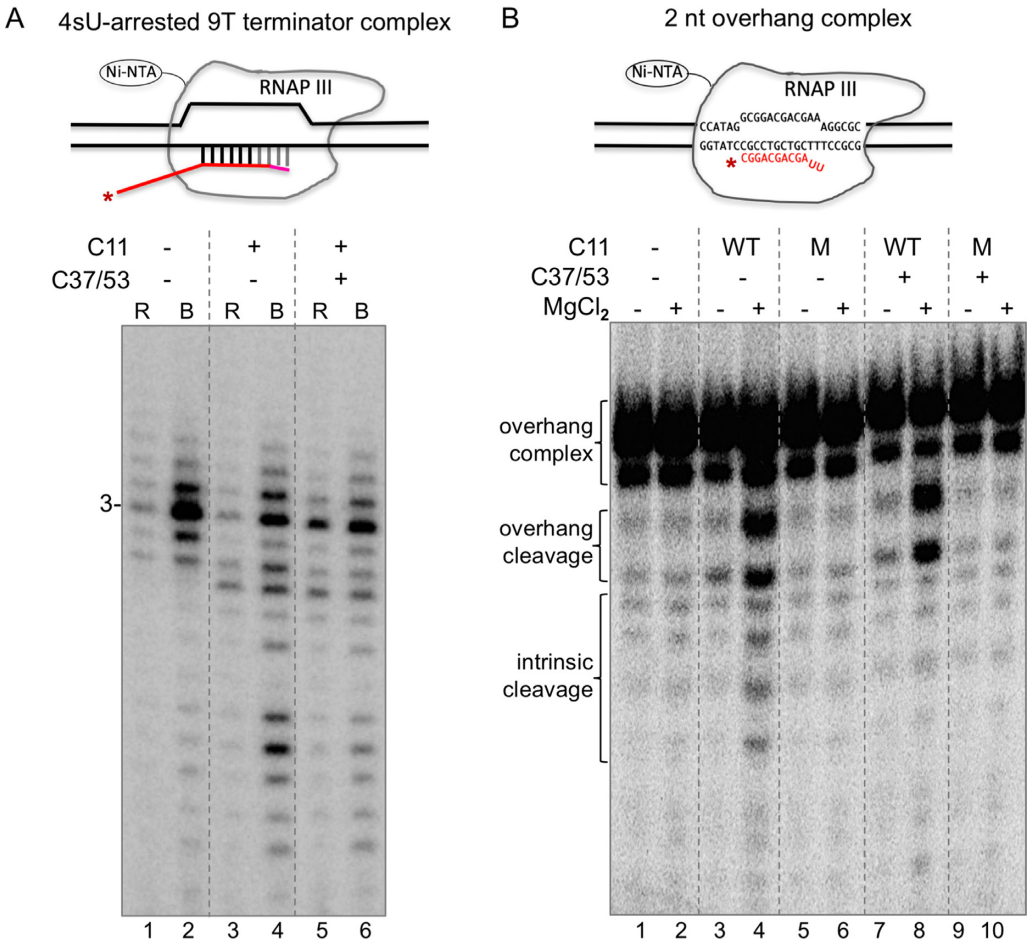

Figure 7. C37/53 can temper C11-stimulated RNA 3′ end cleavage. (**A**) Isolated sU-arrested RNAP III-core complexes on the 9T-9A terminator were washed and incubated with buffer alone or recombinant proteins indicated above the lanes for 30 min in the absence of NTPs, purified and separated into R and B fractions. (**B**) Top: schematic of scaffold assembly of an RNAP III-core EC in a backtracked state in which the 3′ end of the 12-nt RNA has a 2-nt mismatch with the template. This was incubated with either buffer alone or recombinant proteins indicated above the lanes for 15 min prior to addition of $MgCl_2$ as indicated. Total RNA was analyzed without separation of R and B fractions. Cleavage products are indicated by brackets. C11-M is a RNA cleavage-defective form, $C11^{AA}$, as in Figure 2F.

it to 49% (of Figure 8, lanes 9 and 10) as compared to 86.5% arrest with neither C37/53 nor C11 (lanes 3 and 4). By this measure the mutant heterodimers are significantly deficient in preventing arrest (lanes 10–14), albeit with different patterns.

It is worth noting that the mutated heterodimers, C37*/53 and C37/53* were each deficient in TE relative to C37/53 but with distinct patterns reflective of specific defects (26, 29 versus 51%; each with C11, Figure 8A and B lanes 9–14). The C37*/53+C11 pattern was different from C11 alone, most notably in the B fraction at −1 (Figure 8A and B, lane 12 versus lane 6) but was more significantly different from C37/53+C11 (lanes 9–12). Paucity of release at positions 3 and 4 relative to positions 1 and −1 in lane 11 versus 9, shows that substitutions to the C37-CTD loop specifically impaired release at positions 3 and 4.

The patterns of R and B RNAs with mutated C53* were also specific (Figure 8A and B, lanes 13 and 14). Ratios of released RNAs were different for C37/53*+C11 and C37/53+C11; the B fraction revealed a reproducible specific increase in the −1 RNA (Figure 8A and B, lane 14, compare relative amounts of B RNAs at positions 4 and −1 in lanes 14, 12, 10). The data provide evidence that the C37 CTD-loop, the C53-NTD and C11 contribute to active site dynamics during RNAP III elongation and termination. However, because the recombinant proteins did not faithfully reconstitute the TE achieved with the holoenzyme nor the distribution pattern of RNAs produced, the data suggest the possibility that these proteins may lack post-transcriptional modifications or isoforms, or are present in these reactions in relative amounts or in a way(s) that differs from that in RNAP III-holo.

DISCUSSION

The data here significantly advance understanding of transcription termination by RNAP III. First, we defined a minimal terminator for mechanistic studies as 5T on the NT DNA strand and 3A on the DNA template strand (Figure 1). This asymmetry is remarkable and was unexpected. Although previous work suggested the importance of the base specificity of T3-T5 of the terminator (35), the present work demonstrated that a contiguous tract of five Ts is required

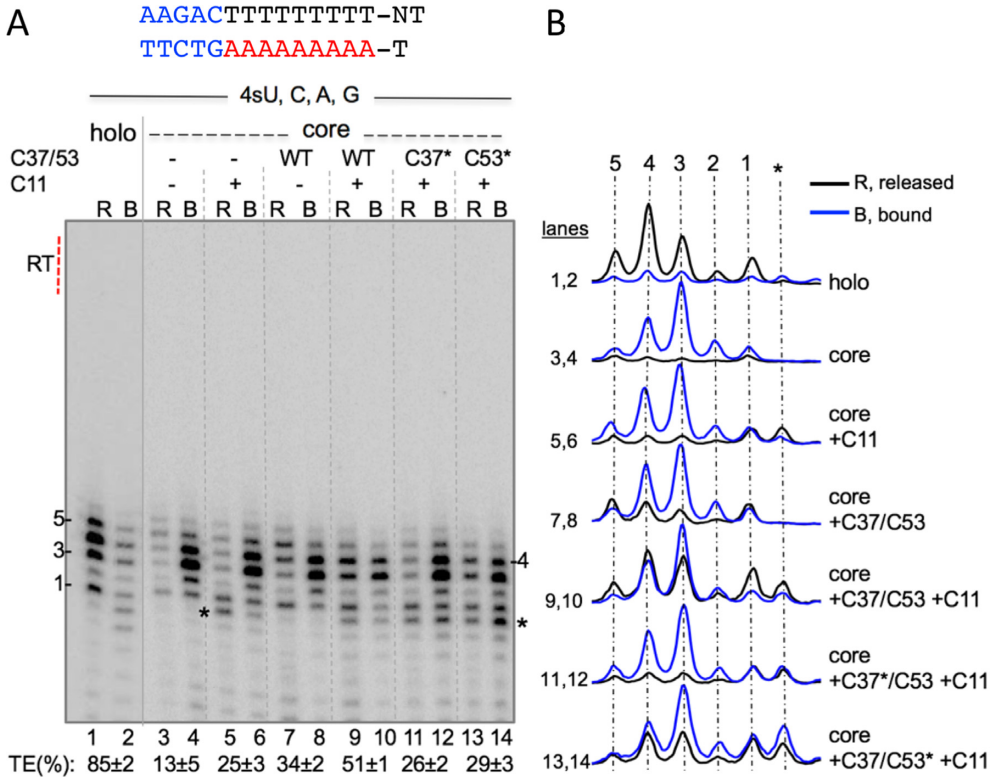

Figure 8. Recombinant C37/53 plus C11 do not faithfully reconstitute RNAP III-core for termination in the 9T-9A terminator with sUTP instead of UTP. (**A**) Transcription on 9T-9A terminator with sU by RNAP III-holo (lanes 1–2), or RNAP III-core and ±C37/53 and C11 as indicated above the lanes (lanes 3–14). (**B**) Quantitative tracings of the lanes of the gel in panel A.

for minimal terminator function. Moreover, it was surprising that fewer As would be required on the template strand than Ts on the NT for termination by RNAP III. It was also surprising that only 3As would be required. Prior evidence suggested dependence on instability of the rU:dA tract (34). That the natural length of most tRNA gene terminators in *S. cerevisiae* of ≥6Ts (42,56) suggested requirement for more instability than contributed by just three rU:dA base pairs. Another novel conclusion is that a major difference in termination between RNAP III-holo and RNAP III-core could be attributed to base pairing strength of the RNA:DNA hybrid and this was revealed by the 5T:3A terminator (Figure 2A–E). Third, the deficiency of RNAP III-core to terminate efficiently on the minimal terminator could be reconstituted with recombinant C37/53 and C11 whether or not the latter was the RNA cleavage active form (Figure 2F). Multiple points distinguishing this conclusion are noteworthy; (i) C37/53 is required for this efficient termination activity; (ii) C37/53 works alone in this capacity to a significant degree whereas by contrast C11 alone has no activity in this termination assay (Figure 2F); (iii) although C11 has no capacity to stimulate termination in the absence of C37/53, its stimulatory effect is relatively very strong (Figure 2F). Because stimulation by C11 is strong even if it is inactive for cleavage, we suspect its effect is mediated via its Rpb9-homologous N-terminal domain which interacts with the dimerization regions of C37/53 and the Rpc2 lobe region at the periphery of the polymerase (26), and in which point mutations are known to alter termination (32). Fourth, the ability of C37/53 to reconstitute a deficiency of RNAP III-core that is attributable to properties of RNA:DNA hybrid stability is a new activity of the heterodimer that has implications beyond RNAP III. Bacterial RNAP controls the RNA:DNA hybrid with its two largest subunits and uses a RNA hairpin component of intrinsic terminators to destabilize the hybrid (52,57,58). Our work here is the first to show that subunits other than the two largest of any multisubunit RNAP contributes to controlling the hybrid toward a major outcome of the transcription cycle. In addition, as the C37/53 heterodimer also participates in initiation, we should suspect that it may use similar activity directed toward the hybrid during that phase of the cycle (24). More generally, because the subunit heterodimer Rpa49/34.5 is related to C53/37 in their dimerization domains, our data suggest that it may exhibit similar activity in RNAP I, at least at certain phases of the transcription cycle. A similar role may be suspected of the TFIIF homolog of C37/53 (59). A fifth and perhaps most striking conclusion is that a major function of C37/53 is to maintain RNA 3′ end engagement with the active site templte while RNAP III is in an oligo(dT) terminator tract, and perhaps while the polymerase traverses other genomic regions of hybrid instability.

Our data demonstrate that RNAP III termination does not occur from the arrested state examined here, even if provided with cleavage-active C11. Rather, we provide evidence that transcription termination proceeds from an active complex whose RNA 3′ end is in the active site. This leads

to a conceptual advance in understanding termination by RNAP III, that while arrest may occur in the oligo-T tract after incorporation of sequential UMP and more so after sequential sUMP, this is rescued by C37/53 RNA:DNA stabilization and rU:dA hybrid 3′ end alignment/annealing activity, *not* by C11 cleavage activity. As detailed below, we believe that without C37/53, the RNA:DNA hybrid becomes destabilized and the 3′ end transiently breathes/melts from the active site template to become arrested in a non-backtracked manner. In this state, what is needed to reset the RNA 3′ end is hybrid stabilization, *not* cleavage. Our data help resolve the roles of C37/53 and C11 in the type of arrest that can occur in a terminator region.

The data also demonstrate that a mutant Rpc53 subunit in a region outside its dimerization domain is clearly deficient. The deficiency of the the C37/53* heterodimer is demonstrated both for the heterodimer's ability to *rescue* sU-arrested complexes (Figure 6A–C) as well as the ability to *prevent* arrest (Figure 8). In addition, the Rpc37 mutant used here is one that had not been examined before, it is a substitution mutant whereas previous mutants in the termination-initiation loop of C37 were deletion mutants (25,35). This mutant, C37*/53 is also deficient in ability to rescue sU-arrested complexes (Figure 6A–C) as well as the ability to prevent arrest (Figure 8).

It was previously noted that RNAP III-core had a propensity to become arrested in the 9T terminator after sequential UMP incorporation (34), intriguing because RNAP III-core exhibits general increased elongation rate relative to the holoenzyme (9). As a result of experiments to examine effects on termination of the UTP analogs, BrUTP and sUTP which strengthen and weaken base pairing, respectively, we discovered that incorporation of sequential sUMPs greatly exacerbated the propensity for arrest by the RNAP III-core but not by RNAP III-holo enzyme (Figure 3A). The striking arrest that occurs after sequential sUMP incorporation by RNAP III-core suggested that the associated weakening of the RNA:DNA hybrid in the absence of C37/53 was a critical determinant of the arrest. As noted, destabilization of the RNA:DNA hybrid in bacterial RNAP led to RNA 3′ end detachment from the active site (47). Our data show that RNAP III lacking C37/53/11 arrests rather than terminates in the proximal part of the 9T tract after sequential sUMP incorporation. Further, the data strongly suggest that RNA 3′ end engagement with the active site is a determinant of termination. As relates to other RNAPs, RNA 3′ end engagement in the active site has not been a specific focus as a determinant of termination other than as in competition with elongation toward read-through (58). Specifically, sU-mediated RNA 3′ end displacement was not found to interfere with termination *per se* by *E. coli* RNAP (47).

Our data robustly show that RNAP III-core is more sensitive to sU-mediated RNA 3′ displacement-mediated arrest than is RNAP III-holo (Figure 3A). Remarkably, the data showed that C37/53 promotes RNA 3′ end polymerase activity of isolated sU pre-termination complexes in elongation reactions. Moreover, C37/53 promoted termination from sU pre-termination complexes in the absence of NTPs, with time course kinetics similar to that in which C37/53 promotes elongation in the early part of the terminator, as well as in the presence of C11 whose RNA 3′ cleavage activity was in competition for the RNA 3′ end.

Involvement of C11 in RNAP III termination

Use of the minimal terminator, 5T-3A showed that C11 strongly stimulates TE by C37/53. Our data indicate that stimulation of TE by C11 is independent of its RNA 3′ cleavage activity in this assay system. A C11 activity that is independent of its RNA 3' cleavage stimulatory activity is somewhat similar to its role in facilitated recycling, a component of which is reportedly dependent on proper termination (9). C11 interacts with C37/53 via its NTD at the lobe region of RNAP III via Rpc2 (Ret1) which impacts termination *in vivo* (26,32,33).

A challenge has been to understand how C11-mediated active site RNA 3′ cleavage is integrated with RNAP III function. Previous data suggest that C11-mediated RNA 3′ cleavage occurs during termination by RNAP III with functional impact on precursor tRNA processing and maturation (31). Our preliminary data suggest that C11-mediated RNA 3′ cleavage can have functional impacts in terminator-specific contexts. A goal of future studies is to determine the extent to which the RNA cleavage activity of the C11-CTD impacts termination.

The termination and associated RNA distribution patterns that we observed suggest that the C11-CTD -mediated RNA cleavage activity is more tempered in RNAP III-holoenzyme than with recombinant C37/53 (see Figure 8). Also, addition of recombinant proteins to RNAP III-core does not fully reconstitute RNAP III-holo activity (34,35). This leaves open the possibility that post-translational modifications that affect RNAP III activity in a C11-dependent regulatory manner (60) may account for discrepancies between native and reconstituted RNAP III.

A model for RNAP III termination

The RNAP III termination bubble is comprised of the oligo(dT) NT strand pause element, with sequence-specific information at T3-T4-T5, and a RNA:DNA hybrid whose stability appears to be affected by the presence of C37/53 which also helps maintain RNA 3′ end engagement/alignment with the template in the active site. The data suggest that RNAP III must detect an unstable hybrid whose RNA 3′ end is in the active site while in a terminator zone, i.e., with T5 on the NT DNA strand, for termination to occur.

Cumulative data from our lab and others have led to what we refer to here as a 'catch and release' model of termination by RNAP III. Comparative analysis of the structures of ECs formed by various RNAPs revealed that RNAP III has an unusually loose RNA:DNA hybrid binding active site and the suggestion that this contributes to efficient termination (26). Specifically, because the termination signal, ≥5Ts, occurs 3′ to but not within the coding sequence of its substrate genes, the loose grip on the terminator RNA:DNA hybrid would allow RNAP III to readily release on cue upon its first encounter with the signal (26). The propensity for RNA 3′ end detachment as hybrid strength decreases may likely reflect the loose binding site for the RNA:DNA hybrid (26).

C37/53 is known to occupy space in the active center ('Introduction' section) and its absence may further loosen the hybrid binding site (61) and thereby account for increased sensitivity of the RNAP III-core to this type of arrest, due to hybrid destabilization.

A weak RNA:DNA duplex can contribute to RNA 3′ end displacement even by a RNAP with a relatively tight hybrid binding site (47). Because tRNA genes tend to have low %G+C in the upstream hybrids preceding their terminators (see 62), one must suspect this to be problematic for RNAP III, i.e., that the RNA 3′ end would transiently wander out of the active site. Without C37/53, the RNA:DNA hybrid would become destabilized and the 3′ end would transiently detach/fray/melt away from the active site template in a non-backtracked manner. In this state, what is needed to reset the RNA 3′ end is hybrid stabilization, not cleavage. However, other pathways to termination by RNAP III may also be possible (53,63). As our data provide compelling evidence that C37/53 can act to reset the RNA 3′ end in the active site, it would be the major factor important for preventing arrest in the terminator region and other sites of low thermal stability of RNA:DNA hybrids. We refer to the presence of C37/53 and its ability to 'catch' such 3′ ends in the early proximal part of an oligo(dT) terminator and help maintain the RNA 3′ end with the active site. However at this proximal stage the hybrid may not have acquired enough instability to signal termination and C37/53 activity would support elongation until the rU:dA hybrid is extended farther into the oligo(dT) tract to become long and unstable enough for termination to occur (37). In this model, termination occurs from a complex with the RNA 3′ end in the RNAP III active site, aided by C37/53.

SUPPLEMENTARY DATA

Supplementary Data are available at NAR Online.

ACKNOWLEDGEMENTS

We thank I. Artsimovitch, M. Kireeva, M. Kashlev, M. Palangat, D. Price and members of the Maraia Lab for discussion and suggestions, and M. Girbig for comments on the manuscript.

Author Contributions': S.M. and R.M. conceived experiments, analyzed raw data and wrote the paper. S.M. performed experiments. R.M. supervised.

FUNDING

Eunice Kennedy Shriver National Institute of Child Health and Human Development (NICHD) [HD000412-30 PGD]. Funding for open access charge: NICHD [HD000412-30 PGD].

Conflict of interest statement. None declared.

REFERENCES

1. Waldron,C. and Lacroute,F. (1975) Effect of growth rate on the amounts of ribosomal and transfer ribonucleic acids in yeast. *J. Bacteriol.*, **122**, 855–865.
2. Ramsay,E.P. and Vannini,A. (2017) Structural rearrangements of the RNA polymerase III machinery during tRNA transcription initiation. *Biochim. Biophys. Acta.*, **1861**, 285–294.
3. Dieci,G. and Sentenac,A. (1996) Facilitated recycling by RNA polymerase III. *Cell* **84**, 245–252.
4. Arimbasseri,A.G., Rijal,K. and Maraia,R.J. (2014) Comparative overview of RNA polymerase II and III transcription cycles, with focus on RNA polymerase III termination and reinitiation. *Transcription* **5**, e27639.
5. Khoo,S.K., Wu,C.C., Lin,Y.C., Lee,J.C. and Chen,H.T. (2014) Mapping the protein interaction network for TFIIB-related factor Brf1 in the RNA polymerase III preinitiation complex. *Mol. Cell. Biol.* **34**, 551–559.
6. Wei,Y.Y. and Chen,H.T. (2017) Functions of the TFIIE-related tandem winged-helix domain of Rpc34 in RNA polymerase III initiation and elongation. *Mol. Cell. Biol.*, **38**, e00105-17.
7. Kuhn,C.D., Geiger,S.R., Baumli,S., Gartmann,M., Gerber,J., Jennebach,S., Mielke,T., Tschochner,H., Beckmann,R. and Cramer,P. (2007) Functional architecture of RNA polymerase I. *Cell* **131**, 1260–1272.
8. Geiger,S.R., Lorenzen,K., Schreieck,A., Hanecker,P., Kostrewa,D., Heck,A.J. and Cramer,P. (2010) RNA polymerase I contains a TFIIF-related DNA-binding subcomplex. *Mol. Cell* **39**, 583–594.
9. Landrieux,E., Alic,N., Ducrot,C., Acker,J., Riva,M. and Carles,C. (2006) A subcomplex of RNA polymerase III subunits involved in transcription termination and reinitiation. *EMBO J.* **25**, 118–128.
10. Chedin,S, Riva,M., Schultz,P., Sentenac,A. and Carles,C. (1998) RNA cleavage activity of RNA polymerase III is mediated by essential TFIIS-like subunit important for transcription termination. *Genes Dev.* **12**, 3857–3871.
11. Appling,F.D., Scull,C.E., Lucius,A.L. and Schneider,D.A. (2018) The A12.2 subunit is an intrinsic destabilizer of the RNA polymerase I elongation complex. *Biophys. J.* **114**, 2507–2515.
12. Appling,F.D., Schneider,D.A. and Lucius,A.L. (2017) Multisubunit RNA polymerase cleavage factors modulate kinetics and energetics of nucleotide Incorporation: An RNA polymerase I case study. *Biochemistry* **56**, 5654–5662.
13. Willis,I.M. (2018) Maf1 phenotypes and cell physiology. *Biochim. Biophys. Acta* **1861**, 330–337.
14. Mange,F., Praz,V., Migliavacca,E., Willis,I.M., Schutz,F., Hernandez,N. and Cycli,X.C. (2017) Diurnal regulation of RNA polymerase III transcription is under the control of both the feeding-fasting response and the circadian clock. *Genome Res.* **27**, 973–984.
15. Bonhoure,N., Byrnes,A., Moir,R.D., Hodroj,W., Preitner,F., Praz,V., Marcelin,G., Chua,S.C. Jr, Martinez-Lopez,N., Singh,R. *et al.* (2015) Loss of the RNA polymerase III repressor MAF1 confers obesity resistance. *Genes Dev.* **29**, 934–947.
16. Filer,D., Thompson,M.A., Takhaveev,V., Dobson,A.J., Kotronaki,I., Green,J.W.M., Heinemann,M., Tullet,J.M.A. and Alic,N. (2017) RNA polymerase III limits longevity downstream of TORC1. *Nature* **552**, 263–267.
17. Chiu,Y.H., Macmillan,J.B. and Chen,Z.J. (2009) RNA polymerase III detects cytosolic DNA and induces type I interferons through the RIG-I pathway. *Cell* **138**, 576–591.
18. Ablasser,A., Bauernfeind,F., Hartmann,G., Latz,E., Fitzgerald,K.A. and Hornung,V. (2009) RIG-I-dependent sensing of poly(dA:dT) through the induction of an RNA polymerase III-transcribed RNA intermediate. *Nat. Immunol.* **10**, 1065–1072.
19. Ogunjimi,B., Zhang,S.Y., Sorensen,K.B., Skipper,K.A., Carter-Timofte,M., Kerner,G., Luecke,S., Prabakaran,T., Cai,Y., Meester,J. *et al.* (2017) Inborn errors in RNA polymerase III underlie severe varicella zoster virus infections. *J. Clin. Invest.* **127**, 3543–3556.
20. Carter-Timofte,M.E., Hansen,A.F., Christiansen,M., Paludan,S.R. and Mogensen,T.H. (2018) Mutations in RNA Polymerase III genes and defective DNA sensing in adults with varicella-zoster virus CNS infection. *Genes Immun.*, **20**, doi:10.1038/s41435-018-0027-y.
21. Bernard,G. and Vanderver,A. (2012) POLR3-Related Leukodystrophy. In: Pagon,RA, Bird,TD, Dolan,CR, Stephens,K and Adam,MP (eds). *GeneReviews*, Seattle, WA.
22. Arimbasseri,A.G. and Maraia,R.J. (2016) RNA Polymerase III advances: structural and tRNA functional views [Review]. *Trends Biochem. Sci.* **41**, 546–559.
23. Ittmann,M., Ali,J., Greco,A. and Basilico,C. (1993) The gene complementing a temperature-sensitive cell cycle mutant of BHK cells is the human homologue of the yeast RPC53 gene, which encodes a subunit of RNA polymerase C (III). *Cell Growth Differ.* **4**, 503–511.

24. Kassavetis,G.A., Prakash,P. and Shim,E. (2010) The C53/C37 subcomplex of RNA polymerase III lies near the active site and participates in promoter opening. *J. Biol. Chem.* **285**, 2695–2706.
25. Wu,C.C., Lin,Y.C. and Chen,H.T. (2011) The TFIIF-like Rpc37/53 dimer lies at the center of a protein network to connect TFIIIC, Bdp1, and the RNA polymerase III active center. *Mol. Cell. Biol.* **31**, 2715–2728.
26. Hoffmann,N., Jakobi,A., Moreno-Morcillo,M., Glatt,S., Kosinski,J., Hagen,W., Sachse,C. and Muller,C. (2015) Molecular structures of unbound and transcribing RNA polymerase III. *Nature* **528**, 231–236.
27. Abascal-Palacios,G., Ramsay,E.P., Beuron,F., Morris,E. and Vannini,A. (2018) Structural basis of RNA Polymerase III transcription initiation. *Nature*, **553**, 301–306.
28. Vorländer,M.K., Khatter,H., Wetzel,R., Hagen,W.J.H. and Muüller,C.M. (2018) Molecular mechanism of promoter opening by RNA polymerase III. *Nature*, **553**, 295–300.
29. Shaaban,S.A., Bobkova,E.V., Chudzik,D.M. and Hall,B.D. (1996) In vitro analysis of elongation and termination by mutant RNA polymerases with altered termination behavior. *Mol. Cell. Biol.* **16**, 6468–6476.
30. Rijal,K. and Maraia,R.J. (2016) Active center control of termination by RNA Polymerase III and tRNA gene transcription levels *in vivo*. *PLoS Genet.* **12**, e1006253.
31. Huang,Y., Intine,R.V., Mozlin,A., Hasson,S. and Maraia,R.J. (2005) Mutations in the RNA polymerase III subunit Rpc11p that decrease RNA 3′ cleavage activity increase 3′-Terminal Oligo(U) length and la-dependent tRNA processing. *Mol. Cell. Biol.* **25**, 621–636.
32. Iben,J.R., Mazeika,J.K., Hasson,S., Rijal,K., Arimbasseri,A.G., Russo,A.N. and Maraia,R.J. (2011) Point mutations in the Rpb9-homologous domain of Rpc11 that impair transcription termination by RNA polymerase III. *Nucleic Acids Res.* **39**, 6100–6113
33. Rijal,K. and Maraia,R.J. (2013) RNA polymerase III mutants in TFIIFα-like C37 cause terminator readthrough with no decrease in transcription output. *Nucleic Acids Res.* **41**, 139–155.
34. Arimbasseri,A.G. and Maraia,R.J. (2013) Distinguishing core and holoenzyme mechanisms of transcription termination by RNA polymerase III. *Mol. Cell. Biol.* **33**, 1571–1581.
35. Arimbasseri,A.G. and Maraia,R.J. (2015) Mechanism of transcription termination by RNA polymerase III utilizes a non-template strand sequence-specific signal element. *Mol. Cell* **58**, 1124–1132.
36. Martin,F.H. and Tinoco,I. Jr (1980) DNA-RNA hybrid duplexes containing oligo(dA:rU) sequences are exceptionally unstable and may facilitate termination of transcription. *Nucleic Acids Res.* **8**, 2295–2299.
37. von Hippel,P.H. and Yager,T.D. (1992) The elongation-termination decision in transcription. *Science* **255**, 809–812.
38. Maraia,R.J. and Rijal,K. (2015) Structural biology: a transcriptional specialist resolved. *Nature* **528**, 204–205.
39. Nudler,E. (2012) RNA polymerase backtracking in gene regulation and genome instability. *Cell* **149**, 1438–1445.
40. Arimbasseri,A.G., Kassavetis,G.A. and Maraia,R.J. (2014) Comment on "Mechanism of eukaryotic RNA polymerase III transcription termination". *Science* **345**, 524.
41. Hamada,M., Sakulich,A.L., Koduru,S.B. and Maraia,R. (2000) Transcription termination by RNA polymerase III in fission yeast: a genetic and biochemical model system. *J. Biol. Chem.* **275**, 29076–29081.
42. Braglia,P., Percudani,R. and Dieci,G. (2005) Sequence context effects on oligo(dT) termination signal recognition by Saccharomyces cerevisiae RNA polymerase III. *J. Biol. Chem.* **280**, 19551–19562.
43. Kettenberger,H., Armache,K.J. and Cramer,P. (2004) Complete RNA polymerase II elongation complex structure and its interactions with NTP and TFIIS. *Mol. Cell* **16**, 955–965.
44. Cheung,A.C., Sainsbury,S. and Cramer,P. (2011) Structural basis of initial RNA polymerase II transcription. *EMBO J.* **30**, 4755–4763.
45. Miller,C., Schwalb,B., Maier,K., Schulz,D., Dumcke,S., Zacher,B., Mayer,A., Sydow,J., Marcinowski,L., Dolken,L. *et al.* (2011) Dynamic transcriptome analysis measures rates of mRNA synthesis and decay in yeast. *Mol. Syst. Biol.* **7**, 458.
46. Tani,H. and Akimitsu,N. (2012) Genome-wide technology for determining RNA stability in mammalian cells: historical perspective and recent advantages based on modified nucleotide labeling. *RNA Biol.* **9**, 1233–1238.
47. Nudler,E., Mustaev,A., Lukhtanov,E. and Goldfarb,A. (1997) The RNA-DNA hybrid maintains the register of transcription by preventing backtracking of RNA polymerase. *Cell* **89**, 33–41.
48. Core,L.J., Waterfall,J.J. and Lis,J.T. (2008) Nascent RNA sequencing reveals widespread pausing and divergent initiation at human promoters. *Science* **322**, 1845–1848.
49. Toulokhonov,I., Zhang,J., Palangat,M. and Landick,R. (2007) A central role of the RNA polymerase trigger loop in active-site rearrangement during transcriptional pausing. *Mol. Cell* **27**, 406–419.
50. Artsimovitch,I. and Landick,R. (2000) Pausing by bacterial RNA polymerase is mediated by mechanistically distinct classes of signals. *Proc. Natl. Acad. Sci. U.S.A.* **97**, 7090–7095.
51. Sydow,J.F., Brueckner,F., Cheung,A.C., Damsma,G.E., Dengl,S., Lehmann,E., Vassylyev,D. and Cramer,P. (2009) Structural basis of transcription: mismatch-specific fidelity mechanisms and paused RNA polymerase II with frayed RNA. *Mol. Cell* **34**, 710–721.
52. Gusarov,I. and Nudler,E. (1999) The mechanism of intrinsic transcription termination. *Mol. Cell* **3**, 495–504.
53. Ray-Soni,A., Mooney,RA. and Landick,R. (2017) Trigger loop dynamics can explain stimulation of intrinsic termination by bacterial RNA polymerase without terminator hairpin contact. *Proc. Natl. Acad. Sci. U.S.A.* **114**, E9233–E9242.
54. Lubkowska,L., Maharjan,A.S. and Komissarova,N. (2011) RNA folding in transcription elongation complex: implication for transcription termination. *J. Biol. Chem.* **286**, 31576–31585.
55. Mishra,S. and Sen,R. (2015) N protein from lambdoid phages transforms NusA into an antiterminator by modulating NusA-RNA polymerase flap domain interactions. *Nucleic Acids Res.* **43**, 5744–5758.
56. Iben,J.R. and Maraia,R.J. (2012) Yeast tRNAomics: tRNA gene copy number variation and codon use provide bioinformatics evidence of a new wobble pair in a eukaryote. *RNA* **18**, 1358–1372.
57. Ray-Soni,A., Bellecourt,M.J. and Landick,R. (2016) Mechanisms of bacterial transcription termination: all good things must end. *Annu. Rev. Biochem.* **85**, 319–347.
58. Peters,J.M., Vangeloff,A.D. and Landick,R. (2011) Bacterial transcription terminators: the RNA 3′-end chronicles. *J. Mol. Biol.* **412**, 793–813.
59. Carter,R. and Drouin,G. (2010) Increase in number of subunits in eukaryotic RNA polymerase III relative to RNA polymerase II is due to permanent recruitment of general transcription factors. *Mol. Biol. Evol.* **27**, 1035–1043.
60. Lee,J., Moir,R.D., McIntosh,K.B. and Willis,I.M. (2012) TOR signaling regulates ribosome and tRNA synthesis via LAMMER/Clk and GSK-3 family kinases. *Mol. Cell* **45**, 836–843.
61. Hoffmann,N.A., Jakobi,A.J., Vorlander,M.K., Sachse,C. and Muller,C.W. (2016) Transcribing RNA polymerase III observed by electron cryo-microscopy. *FEBS J.*, **2811**, 2811–2819.
62. Lee,Y., Kindelberger,D.W., Lee,J.Y., McClennen,S., Chamberlain,J. and Engelke,D.R. (1997) Nuclear pre-tRNA terminal structure and RNase P recognition. *RNA* **3**, 175–185.
63. Komissarova,N., Becker,J., Solter,S., Kireeva,M. and Kashlev,M. (2002) Shortening of RNA:DNA hybrid in the elongation complex of RNA polymerase is a prerequisite for transcription termination. *Mol. Cell* **10**, 1151–1162.